Title:

Therapeutic KRAS^{G12C} inhibition drives effective interferon-mediated anti-tumour immunity in immunogenic lung cancers

Authors:

Edurne Mugarza[1,†], Febe van Maldegem[1,4,†], Jesse Boumelha[1], Christopher Moore[1], Sareena Rana[1], Miriam Llorian Sopena[2], Philip East[2], Rachel Ambler[1], Panos Anastasiou[1], Pablo Romero Clavijo[1], Karishma Valand[1], Megan Cole[1], Miriam Molina-Arcas[1,*], Julian Downward[1,3,*]

Affiliations:

[1] Oncogene Biology Laboratory, Francis Crick Institute, 1 Midland Road, London NW1 1AT, UK

[2] Bioinformatics and Biostatistics Science Technology Platform, Francis Crick Institute, 1 Midland Road, London NW1 1AT, UK

[3] Lung Cancer Group, Division of Molecular Pathology, Institute of Cancer Research, 237 Fulham Road, London SW3 6JB, UK.

[4] Present address: Department of Molecular Cell Biology and Immunology, Amsterdam UMC, Location VUMC, De Boelelaan 1108, 1081HZ Amsterdam, The Netherlands

[†] These authors contributed equally

[*] Correspondence: julian.downward@crick.ac.uk , miriam.molina@crick.ac.uk

One sentence summary:

KRAS^{G12C} inhibition mobilizes anti-tumour immunity in immunogenic lung cancer models through derepressing interferon signaling via repression of Myc.

Abstract:

The recent development and approval of $KRAS^{G12C}$ inhibitors promises to change profoundly the clinical management of lung cancer patients harbouring $KRAS^{G12C}$ mutations. However, early clinical data indicate that acquired drug resistance can frequently develop after the initial response. Due to the immunosuppressive nature of the signaling network controlled by oncogenic KRAS, targeted $KRAS^{G12C}$ inhibition can indirectly affect anti-tumour immunity. This has served as a rationale for combination with immune checkpoint blockade, showing therapeutic benefit in certain immunogenic pre-clinical tumour models. In this study, we characterised how $KRAS^{G12C}$ inhibition reverses immune suppression driven by oncogenic KRAS in a number of pre-clinical lung cancer models with varying levels of immunogenicity. Mechanistically, $KRAS^{G12C}$ inhibition upregulates interferon pathway gene expression via inhibition of Myc and, in tumours, leads to reduced infiltration of immunosuppressive cells, increased interferon responses and antigen presentation, and also enhanced infiltration and activation of cytotoxic T cells. However, the combination of $KRAS^{G12C}$ inhibitors with immune checkpoint blockade only provides synergistic benefit in the most immunogenic tumour model, with $KRAS^{G12C}$ inhibition failing to sensitize cold tumours to immunotherapy. In immunogenic tumours, complete responses to $KRAS^{G12C}$ inhibition requires tumour cell autonomous interferon γ signaling. Our data have important implications for the design of clinical trials combining $KRAS^{G12C}$ inhibitors with anti-PD-1 drugs and suggest that additional combination strategies will be needed for immunotherapy refractory patients.

Main text:

INTRODUCTION

Lung cancer is the number one cause of cancer deaths worldwide, leading to some 1.8 million deaths annually, and therefore represents a disease of very high unmet need (*1*). Non-small cell lung cancer (NSCLC) comprises 84% of all lung cancers and has a 5-yr survival rate of only 25% (*2*). Fortunately, with the introduction of immune checkpoint blockade (ICB), aiming to boost anti-tumour T cell immunity, the paradigm for treatment has shifted, enabling long-lasting responses in a subset of patients (*3*). However, only a minority of patients respond and, of those that do, many develop resistance to treatment over time, hence great efforts are currently aimed at trialing therapeutic combinations with ICB (*4*). Targeting oncogenic drivers has been another approach to control tumour growth, as recurrent genetic alterations are detected in more than half of lung adenocarcinoma patients (*5*). Targeted inhibition of receptor tyrosine kinases such as EGFR has extended progression-free survival beyond conventional cytotoxic therapies. But, until recently, inhibiting KRAS, the most frequent target of oncogenic mutations found in about 15% of all cancer patients and 33% of those with lung adenocarcinoma (*6*), has been notoriously difficult. In 2013, Ostrem et al. reported the development of a covalent inhibitor that was able to lock KRAS into its inactive GDP-bound state by binding to the cysteine resulting from the G12C mutation, present in 40% of KRAS-mutant NSCLC patients (*7*). A mutation-specific inhibitor would be able to circumvent the high toxicity that has limited the widespread use of compounds targeting signaling downstream of KRAS, such as MEK inhibitors. The discovery of a $KRAS^{G12C}$-specific compound led to rapid development of clinical inhibitors and in 2021 Amgen was the first to obtain FDA approval for clinical use of AMG510 (Sotorasib) in locally advanced or metastatic $KRAS^{G12C}$-mutant NSCLC (*8-10*). As expected, toxicity from these drugs is low as signaling is only inhibited in cancer cells harboring the G12C mutation, and clinical response rates are high, but unfortunately resistance occurs frequently within a few months of treatment. Several mechanisms of resistance have already been described, including novel mutations in KRAS or bypassing the mutation via redundant signaling pathways (*11-13*). Hence, combination therapies will be needed to make a greater impact on patient survival (*14, 15*).

Exploring the combination of targeted inhibition of KRAS with ICB seems an obvious approach and indeed the first clinical trials are already well underway. There are certainly rational arguments to make for this combination, with KRAS mutant lung cancer generally being associated with a smoking-history and therefore high tumour mutation burden, one of the positive predictors for response to ICB (*16, 17*). Moreover, KRAS-mutant lung cancer is strongly associated with an immune evasive phenotype and KRAS signaling is thought to play a role in orchestrating such an immune suppressive environment, for example by driving the

expression of cytokines and chemokines as was shown for IL-10, TGF-beta and GM-CSF in KRAS mutant pancreatic cancer (*18*). Inhibition of KRAS could provide temporary relief from such immune suppression and a window of opportunity for T cell activation. Indeed, initial reports of $KRAS^{G12C}$ inhibition showed that durable responses in mice were dependent on T cells, and a combination of $KRAS^{G12C}$ inhibition and ICB led to improved survival in a subcutaneous tumour model of the genetically engineered $KRAS^{G12C}$ mutant CT26 colon cancer cell line (*8, 19*). While the $KRAS^{G12C}$ mutation is only found in 3-4% of colon carcinoma, it is more prevalent in NSCLC (~14%) and clinical efficacy of the KRAS inhibitors also seems to be higher in lung cancer (*9*). Therefore, it will be most relevant to understand the mechanisms underlying potential therapeutic cooperation between KRAS inhibition and immune responses in the setting of lung cancer. Tissue site, existing immune evasive tumour microenvironment (TME) and intrinsic immunogenicity in the form of neoantigen presentation are all likely to be important factors in determining the outcome of combination treatments with ICB (*4*). Fedele, et al. showed that a combination of SHP2 and $KRAS^{G12C}$ inhibition led to good tumour control and increased T cell infiltration in an orthotopic model of lung cancer (*20*). Using the strongly immune evasive 3LL ΔNRAS lung cancer cell line (*14*), we recently developed an imaging mass cytometry analysis pipeline which showed that $KRAS^{G12C}$ inhibition was able to induce remodeling of the lung TME (*21*). Here, we use this 3LL ΔNRAS alongside other pre-clinical lung cancer models varying in degree of immunogenicity to perform an in-depth investigation of the impact of $KRAS^{G12C}$ inhibition on the TME and anti-tumour immunity and explore the mechanisms that underly the changes observed. We describe several mechanisms by which tumour-specific KRAS inhibition has direct and indirect effects on the TME, such as reduced expression of chemokines attracting immune suppressive myeloid cells, enhanced uptake of tumour cells by antigen presenting cells, and enhanced intrinsic and extrinsic interferon (IFN) responses. Furthermore, we show that successful combination of $KRAS^{G12C}$ inhibition with ICB is not universal, but rather varies between the models and correlates with immunogenicity, which will have important implications for the selection of patients that may benefit from such combination therapy. In particular, tumours that are refractory to ICB, either due to intrinsic or acquired resistance, may be unlikely to be resensitised by combination with $KRAS^{G12C}$ inhibition alone.

RESULTS

Oncogenic KRAS regulates expression of cytokine and immune regulatory genes in human and murine cell lines

Previous reports have described that KRAS signaling can mediate the expression of cytokines such as IL-8 and GM-CSF in pancreatic cancer models (*22*). We therefore decided to assess the role of oncogenic KRAS signaling in the regulation of the expression of immunomodulatory factors in the lung. For this purpose, we made use of a cell line model of immortalised human lung pneumocytes expressing a tamoxifen inducible oncogenic KRAS protein ($KRAS^{G12V\text{-}ER}$) (*14*) (Fig S1A). Activation of oncogenic KRAS signaling induced the secretion of a number of cytokines and chemokines which could affect the recruitment and polarisation of different immune cells (Fig 1A). To further expand the scope of our investigation we performed whole transcriptome analysis (RNA-Seq) on this model. Results validated the transcriptional induction of myeloid cell modulatory factors IL-8, CXCL1, CCL2, GM-CSF, and several other KRAS regulated cytokines (Fig 1B). Additionally, gene set pathway analysis revealed a KRAS-dependent negative regulation of type I and type II interferon (IFN) responses in lung pneumocytes (Fig 1C and S1B), previously shown to be crucial for anti-tumour immunity and sensitivity to immunotherapy (*23, 24*), which could reflect a mechanism triggered by oncogenic KRAS to promote immune evasion.

We then assessed whether treatment with a therapeutic $KRAS^{G12C}$ inhibitor could reverse these mechanisms. In two $KRAS^{G12C}$-mutant human lung cancer cell lines, abrogation of oncogenic KRAS signaling by a $KRAS^{G12C}$ inhibitor (Fig S1C) led to the downregulation of cytokines and chemokines, particularly those involved in the recruitment and differentiation of myeloid cell populations, known to exert tumour-promoting effects in the tumour microenvironment (Fig 1D and S1D top). Interestingly, only the neutrophil chemoattractants CXCL2 and CXCL8 were consistently KRAS-regulated in both models, while most factors were cell line-specific, suggesting that different cell lines exhibit different cytokine expression patterns. RNA-Seq analysis of these cell lines also revealed that $KRAS^{G12C}$ inhibition upregulates IFNα and IFNγ response gene expression, a mechanism that was consistent across both cell lines (Fig 1E and S1D bottom).

We decided to extend our findings to a murine cell line in order to use immunocompetent mouse models to examine the effects of oncogenic KRAS on anti-tumour immunity in vivo. We made use of a murine transplantable $KRAS^{G12C}$-mutant lung cancer cell line derived from Lewis Lung Carcinoma, 3LL ΔNRAS (described in (*14*)), which is sensitive to $KRAS^{G12C}$ inhibition ((*14*), Fig S1E). Using this model, we validated the effect of $KRAS^{G12C}$ inhibitors on the transcriptomic downregulation of secreted immunomodulatory factors, by both RNA-Seq (Fig

1F) and qPCR (Fig S1F) analysis. Likewise, we validated the upregulation of type I and II IFN gene sets observed in previous models (Fig 1G and S1G).

Together, these data suggest that oncogenic KRAS signaling regulates the expression of factors that could affect the tumour microenvironment and anti-tumour immunity and highlight the role of $KRAS^{G12C}$ inhibitors in reversing these potentially immune evasive mechanisms.

KRAS signaling downregulates IFN pathway gene expression via MYC

Next, we decided to further investigate the mechanistic link between KRAS signaling and IFN responses given their important role in anti-tumour immunity. We began by validating our RNA-Seq finding that genes coding for components of the IFN response were upregulated by $KRAS^{G12C}$ inhibition in 3LL ΔNRAS cells (Fig 2A). This upregulation occurred in a MEK-dependent manner, beginning at approximately 6h after treatment and peaking at 24h after treatment (Fig S2A and B). To extend our findings we used two additional mouse cell lines modified to harbor $KRAS^{G12C}$ mutations, the KRAS mutant, p53 deleted lung cancer cell line $KPB6^{G12C}$ (*25*) and the KRAS mutant colon cancer cell line $CT26^{G12C}$ (*19*). In these models, treatment with the $KRAS^{G12C}$ inhibitor MRTX1257 (MRTX) consistently led to the upregulation of canonical IFN signaling pathway genes (Fig 2B).

The conserved regulation of IFN signaling pathway genes after KRAS inhibition could suggest a direct crosstalk between oncogenic KRAS and IFN signaling pathways. IFNs bind their receptors on the membrane of target cells and drive transcriptional changes via activation of JAK-STAT signaling modules. To investigate whether the increase in gene expression in response to KRAS inhibition was a result of augmented IFN signaling, we examined the effect of blocking or depleting individual IFN pathway components. However, antibody-mediated blocking of the IFNα receptor (Fig S2C), pharmacological inhibition of JAK1/2 signal transduction with ruxolitinib (Fig S2D) and gene knockdown of Stat1 or Stat2 (Fig S2E) did not affect the MRTX-driven upregulation of IFN genes (Fig S2F), suggesting that KRAS-driven inhibition of the IFN pathway occurs independently of the interferon receptors and JAK-STAT proteins.

A known negative transcriptional regulator of IFN genes is the MYC oncoprotein, which is also a RAS target (*26*). As expected, MYC mRNA levels were downregulated by $KRAS^{G12C}$ inhibition in vitro and in vivo and upregulated after $KRAS^{G12V}$ activation (Fig 2C and D), confirming the KRAS-driven regulation of MYC in our models. We assessed the role of MYC in the regulation of IFN signaling pathway genes by the $KRAS^{G12C}$ inhibitor. In the 3LL ΔNRAS cell line, despite incomplete knockdown (Fig 2E), MYC depletion was able to significantly increase the expression of these genes (Fig 2F). Because MRTX treatment led to a further downregulation of MYC, increased gene expression was observed when MRTX and siMyc were combined. Importantly, upregulation of IFN signaling pathway genes in response to MYC

depletion was a common response observed across the three murine KRAS^{G12C} cell lines (Fig S2G and S2H). Furthermore, in CT26^{G12C} and KPB6^{G12C} cells, where near-complete knockdown of MYC was achieved (Fig S2G), no significant additional effects on gene or protein expression were observed by combined siMyc and MRTX treatment (Fig 2G), suggesting that MRTX-driven regulation of these genes is primarily through MYC. Together, these data suggests that KRAS^{G12C} inhibition, through downregulation of MYC, leads to increased expression of genes associated with the IFN response.

KRAS^{G12C} inhibition enhances tumour cell intrinsic IFN responses

We next investigated whether KRAS^{G12C} inhibitor-driven changes in gene expression affected the capacity of tumour cells to respond to IFNγ. We found that, indeed, IFNγ-driven transcriptional effects were enhanced by MRTX treatment (Fig 3A). KRAS^{G12C} inhibition augmented the IFNγ-driven expression of immunomodulatory IFN-stimulated genes (ISG) such as T cell chemoattractants *Cxcl9/10/11* and antigen presentation genes including *H2-d/k1*, *Ciita* and *B2m* (Fig 3A and S3A). Consistent with the KRAS-dependent regulation of type I and II IFN responses observed in our RNA-Seq analysis, MRTX treatment was likewise able to enhance IFNα and IFNβ-driven gene expression (Fig S3B). These transcriptional changes also led to increased protein expression of ISG, as evidenced by an increased proportion of IFNγ-induced CXCL9-secreting tumour cells after treatment with MRTX (Fig 3B). We validated that MRTX treatment enhanced IFNγ-driven gene (Fig 3C) and protein (Fig S3C) expression in two additional murine cell lines. A similar improvement of responses to IFNγ could be achieved by MYC knockdown (Fig 3D), confirming the role of MYC in the regulation of IFN responses.

To exclude the possibility that reduced cell fitness contributed to the effects of KRAS^{G12C} inhibition on the response to IFNγ, we validated our findings in the KRAS$^{G12V\text{-}ER}$ human pneumocyte cell line. In this model, we observed that 4-OHT-induced KRAS^{G12V} activation led to the downregulation of IFN signaling pathway genes and was able to decrease IFNγ-driven transcriptional effects (Fig 3E), suggesting a mechanistic link between the KRAS and IFN pathways which is not influenced by cell viability.

In summary, we have shown that oncogenic KRAS signaling can suppress responses to IFN, and that this can be alleviated with pharmacological KRAS^{G12C} inhibition. KRAS inhibition in consequence leads to an increased sensitivity of tumour cells to type I and II IFNs, which translates to higher expression of IFN-induced genes such as T cell chemoattractants and antigen presentation genes that could positively affect anti-tumour immunity in vivo.

KRAS^{G12C} inhibition in vivo remodels the highly immunosuppressive TME of 3LL ΔNRAS lung tumours

The results presented above demonstrate the ability of KRAS^{G12C} inhibitors to reverse KRAS-driven immune evasion mechanisms, such as enhancing tumour cell-intrinsic IFN responses and modulating the expression of secreted immunomodulatory factors. Next, we aimed to assess how inhibition of oncogenic KRAS in vivo can affect the composition of the tumour microenvironment (TME) in lung tumours.

The 3LL ΔNRAS cell line can form orthotopic tumours in the lungs of C57BL/6 mice when delivered intravenously. Immunophenotypic characterisation of these tumours revealed a predominant infiltration of myeloid cells, known to exert immunosuppressive actions, while anti-tumorigenic cells like lymphocytes and NK cells were largely absent from the TME (Fig 4A). Using Imaging Mass Cytometry (IMC) we recently showed that there was an inclusion of macrophages and neutrophils in the core of 3LL ΔNRAS lung tumours, while effector cells remained at the tumour periphery (*21*). Consistent with this apparent immunosuppressive TME, growth of these tumours was not affected by a lack of B and T cells in Rag1$^{-/-}$ mice (Fig S4A). Whole exome sequencing of two 3LL ΔNRAS single cell clones derived from the CRISPR-Cas9 deletion of NRAS (*14*) revealed that these cell lines harbor thousands of clonal somatic nonsynonymous single nucleotide variations (SNVs) compared to the reference C57BL/6J genome (Fig 4B). Whole exome sequencing and RNA expression data were combined to perform in silico neoantigen prediction. Results showed that this cell line harbors numerous predicted neoepitopes with high or medium affinity for MHC binding (Fig S4B) but flow cytometric analysis revealed that it has lost the expression of one of the MHC alleles, H2-Kb, while retaining the other, H2-Db (Fig S4C), possibly reflecting a mechanism to escape immunological rejection. It is noticeable that neoantigens predicted to bind to the absent H2-Kb are several-fold more highly represented than neoantigens precited to bind to the expressed H2-Db. Therefore, we hypothesize that this cell line contains sufficient neoantigens to elicit an anti-tumour immune response, yet it is highly immune evasive and avoids rejection in immunocompetent hosts, likely through a combination of mechanisms including reduced neoantigen presentation and production of an immunosuppressive tumour microenvironment.

Treatment of 3LL ΔNRAS lung tumour-bearing mice with the KRAS^{G12C} inhibitor MRTX1257 for one week resulted in marked tumour growth inhibition (Fig 4C), although relatively few tumours actually decreased in size, highlighting the extreme aggressiveness of this tumour model. At this time point, we harvested tumours to perform RNA-Seq analysis, flow cytometric analysis of immune cell infiltration and IMC to examine the effects of KRAS^{G12C} inhibition on the TME of this highly immunosuppressive model. As anticipated from the in vitro data, gene set enrichment analysis of 3LL ΔNRAS lung tumours treated with MRTX revealed

an upregulation of several immune-related pathways, including interferon α and γ responses, IL2 and IL6 signaling, allograft rejection, complement and inflammatory responses (Fig 4D). We were likewise able to confirm the KRAS-dependent regulation of IFN signaling pathway gene sets in vivo (Fig S4D). This striking remodeling of the TME was confirmed by IMC analysis, where hierarchical clustering based on immune cell infiltration patterns was able to discern vehicle and MRTX-treated samples (Fig 4E).

KRAS^{G12C} inhibition was able to significantly reduce the high infiltration of myeloid cells like monocytes and neutrophils observed in this lung tumour model, as measured by flow cytometry (Fig 4F). We then wondered whether the downregulation of tumour cell-intrinsic cytokine expression observed in vitro (Fig 1F) could play a role in the regulation of myeloid cell infiltration. The strongest KRAS-regulated cytokine in the 3LL ΔNRAS cells in vitro was *Ccl2*, a canonical chemoattractant for monocytes. The KRAS-dependent regulation of CCL2 secretion was also validated in our KRAS$^{G12V\text{-}ER}$ pneumocyte cell line (Fig S4E). Furthermore, in vivo MRTX treatment of 3LL ΔNRAS tumour-bearing mice led to a significant downregulation of *Ccl2* expression in the tumour (Fig 4G), suggesting that tumour cells may be one of the main sources of this cytokine in the TME. To validate the role of KRAS-mediated regulation of CCL2 in the changes observed in the TME, we measured monocyte migration ex vivo. Results showed that migration was significantly abrogated when bone marrow-derived monocytes were cultured in conditioned medium from MRTX-treated cells and to a similar extent when cultured in medium from C*cl2*$^{-/-}$ cells (Fig 4H). This data suggests that tumour cell specific KRAS^{G12C} inhibition, via inhibition of the secretion of CCL2, leads to an impaired recruitment of monocytes into the TME, which could constitute a mechanism that alleviates immunosuppression.

KRAS^{G12C} inhibition in vivo increases T cell infiltration and activation

While a reduction in immunosuppressive populations in the TME constitutes a mechanism to improve anti-tumour immunity, immunological rejection can only be achieved by the specific activation of cytotoxic populations such as CD8+ T cells.

For the generation of an adaptive immune response, lymphocytes need to be primed by professional antigen presenting cells (APC), which in turn need to have been activated themselves by engulfment of tumour-specific antigens. Therefore, we sought to assess if the reduction of viability and increase of apoptosis caused by KRAS^{G12C} inhibition ((*14*) and Fig S1E) could affect dendritic cell (DC) activity in vitro. Indeed, the GFP+ Mutu DCs were able to phagocytose MRTX-treated CellTrace Violet (CTV) labelled 3LL ΔNRAS cells when co-cultured (Fig 5A), which constitutes the first step of DC activation. In addition, we found that in vivo MRTX-treatment increased the presence of APCs in the TME (Fig 5B), with a consistent increase in the expression of genes involved in antigen presentation (Fig 5C, S5A). Consistent with this finding, co-culture of tumour cells with DCs revealed that KRAS^{G12C} inhibition

promoted the upregulation of activation markers MHCII and CD86 on DCs (Fig 5D). Interestingly MHC II upregulation seemed to be mediated by tumour cell secreted factors, while CD86 required the presence of tumour cells, suggesting that different mechanisms might be at play in the tumour cell-mediated activation of DCs (Fig S5B).

Activated DCs are known to secrete CXCR3 ligands (CXCL9/10/11), a prominent feature of inflamed TMEs (*27*). We found that $KRAS^{G12C}$ inhibition in vivo resulted in a higher expression of these T cell chemoattractants and their receptor (Fig 5E, Fig S5C). IMC analysis in the 3LL ΔNRAS lung tumours revealed that CXCL9 was mainly expressed in cells that also expressed markers for APCs (Fig S5D). Furthermore, while these tumours had negligible basal CXCL9 expression, CXCL9-expressing cells were mostly found among dendritic cells and macrophages in a subset of the MRTX treated tumours (Fig 5F). Mechanistically, we observed that the co-culture with MRTX-treated tumour cells was able to lead to the upregulation of CXCL9 in DCs in vitro (Fig 5G). This could not be recapitulated by conditioned medium incubation, suggesting that signals from MRTX-treated tumour cells, other than secreted factors, mediate this upregulation (Fig S5E).

Next, we evaluated whether the observed activation of APCs coincided with changes in the T cell compartment. We observed that the presence of all T cell compartments, particularly Foxp3+ Tregs was increased by MRTX in these lung tumours (Fig 5H). Consistent with the increased T cells, cytotoxicity genes were also significantly upregulated in MRTX-treated tumours (Fig 5I). Interestingly, NK cell infiltration was also increased in treated tumours (Fig S5F) which could be contributing to the increased expression of cytotoxicity genes. This increase in cytotoxicity was confirmed by the significantly increased presence of CD69+ and antigen-experienced (effector and memory) CD8+ T cells observed after MRTX treatment (Fig 5J and S5G).

Previous reports have shown that KRAS inhibition triggers an improved immune response that drives T cell exhaustion, resulting in sensitivity to immune checkpoint blockade (ICB) in immunogenic models of $KRAS^{G12C}$-mutant cancer (*8, 19*) . In our immune evasive 3LL ΔNRAS lung tumour model, we also observed via flow cytometry that PD-1+ T cells were significantly increased after MRTX treatment (Fig S5H). A subset of these cells also expressed LAG-3 (Fig 5K) and we likewise found an upregulation of several other T cell exhaustion genes in our RNA-Seq analysis (Fig S5I).

As CXCL9 expression by DCs was previously described to be crucial to attract effector T cells (*27*), we further explored the relationship between the CXCL9+ DCs and the presence of different T cell subsets in the MRTX-treated tumours. There was a clear correlation between the abundance of CXCL9+ DCs and CD8+ T cells expressing PD-1 and LAG-3 as well as Tregs (Fig S6J). Using the spatial information captured by IMC, we could also see that these

cells are regularly found in close proximity to each other, with a clear enrichment of regulatory T cells and CD8+ T cells with an exhausted phenotype in the direct neighbourhood of CXCL9+ DCs compared to CXCL9- DCs (Fig 5L and 5M). Whether the CXCL9 expressing dendritic cells indeed play a role in recruiting these effector cells, or that activated T cells locally produce IFNγ that in turn induces the CXCL9 expression in the dendritic cells, cannot be deduced from this data.

Together, this data shows that tumour cell-specific KRAS^{G12C} inhibition in a mouse lung cancer model leads to a more inflamed TME, evidenced by an activation of APCs and a strong increase in the presence of activated T cells that could exert cytotoxic actions on the tumour cells, but also display an exhausted phenotype.

KRAS^{G12C} inhibition synergizes with checkpoint blockade only in intrinsically immunogenic tumours

An increased presence of exhausted T cells and augmented IFN responses suggest that MRTX treatment has the potential to sensitize these tumours to ICB. Nevertheless, in this immune-resistant model (*28*), addition of an anti-PD-1 antibody (Fig 6A) or a combination of anti-PD-L1 and anti-LAG3 antibodies (Fig S6A) did not improve the response to KRAS^{G12C} inhibition alone, nor did it enhance the TME remodeling driven by KRAS^{G12C} inhibition (Fig 6B).

To extend our findings, we made use of the KPB6^{G12C} cell line, which has been established from the KRAS$^{LSL_G12D/+}$;Trp53$^{fl/fl}$ mice (KP) and genetically engineered to express a KRAS^{G12C} mutation (*25*). Due to the low number of clonal somatic SNVs, this model develops immune cold lung tumours (*25*). Orthotopic KPB6^{G12C} lung tumours were highly sensitive to KRAS^{G12C} inhibition (Fig S6E). Treatment of KPB6^{G12C} lung tumour-bearing mice with MRTX for a week led to increased T cell infiltration into the tumours (Fig 6C) accompanied by an upregulation of immune genes (Fig 6D). Similar to our findings in 3LL ΔNRAS, we found a significant increase in CD8+ T cell and Tregs and increased *Ifng* and *Gzmb* expression, suggesting increased cytotoxicity. However, in this alternative immune resistant model, no synergism occurred between KRAS^{G12C} inhibition and ICB, and mice in all treatment groups succumbed to disease (Fig 6E). We therefore concluded that despite the profound TME remodeling triggered by KRAS^{G12C} inhibition, it may not be sufficient to render highly immune resistant tumours sensitive to ICB.

We therefore investigated the effects of KRAS^{G12C} inhibition in a new immunogenic model of KRAS-mutant lung cancer. The KPAR^{G12C} cell line has been shown to be immunogenic as its growth is impaired by the adaptive immune system (*25*). Treatment of subcutaneous KPAR^{G12C}-tumour bearing mice with a KRAS^{G12C} inhibitor resulted in outstanding tumour control, with two out of seven mice achieving complete responses (Fig 7A). These responders

were also resistant to tumour re-challenge, suggesting the development of immune memory. In contrast, treatment of 3LL ΔNRAS tumour-bearing mice in the same setting was not able to yield long-term responses, with all mice relapsing on treatment (Fig S7A), reflecting the higher immunogenicity of KPAR^{G12C} tumours. We then assessed the effects of KRAS^{G12C} inhibition on the remodeling of the TME in KPAR^{G12C} lung tumours. Flow cytometric analysis revealed a significant upregulation of activated, antigen-experienced and exhausted T cells (Fig 7B), similar to previous models examined. Treatment with MRTX also led to the upregulation of immune population genes (*Cd8*, *Foxp3*), T cell activation and cytotoxicity genes (*Gzmb*, *Pdcd1*) and IFN response/antigen presentation genes (Fig 7C and S7B). In this immunogenic model, where early treatment with anti-PD-1 alone confers therapeutic benefit (Fig 7D), treatment of orthotopic tumour-bearing mice with MRTX alone led to complete responses in 28% of the mice (Fig 7E). Furthermore, the percentage of complete responders was improved (66%) when KRAS^{G12C} inhibition was administered together with anti-PD1 immunotherapy treatment (Fig 7E).

Given the KRAS-dependent regulation of IFN responses, we examined the role of tumour cell-intrinsic IFNγ signaling in the therapeutic effect of KRAS^{G12C} inhibitors. To this end, we generated *Ifngr2*$^{-/-}$ KPAR^{G12C} cells, which are unable to mount an IFNγ response (Fig S7C, S7D). We observed that complete responses to KRAS^{G12C} inhibition in vivo were dependent on tumour cell-intrinsic IFN signaling, as all mice bearing tumours formed by *Ifngr2*$^{-/-}$ KPAR^{G12C} cells relapsed after MRTX treatment (Fig 7F), while their sensitivity to KRAS inhibition in vitro remained unaffected (Fig S7E). Similarly, KRAS target gene *Dusp6* reduction in vivo was comparable in KPAR^{G12C} WT and *Ifngr2*$^{-/-}$ tumours (Fig 7G, left). On the contrary, we observed that in *Ifngr2*$^{-/-}$ tumours, the increase in T cell cytotoxicity (*Prf1*, *Gzmb*) and activation (*Pdcd1*) in response to KRAS^{G12C} inhibition was significantly attenuated, probably contributing to the decreased long-term therapeutic efficacy of the inhibitor in this model.

Together, these data suggest that in an immunogenic tumour, KRAS^{G12C} inhibition can stimulate anti-tumour immunity, drive complete tumour rejection in a subset of mice and sensitize tumours to ICB, resulting in increased complete responses when both treatments are combined. In addition, this process is dependent on the tumour cell-intrinsic ability to respond to IFNγ, which is regulated by KRAS signaling and contributes to long-term therapeutic efficacy of KRAS^{G12C} inhibition.

DISCUSSION

KRAS^{G12C} inhibitors have shown promising clinical activity in KRAS^{G12C}-mutant NSCLC patients (*9, 10*). However, similarly to other targeted therapies, early clinical results indicate that drug resistance frequently arises, resulting in clinical relapses (*11, 12*). KRAS^{G12C} inhibitors not only affect the survival of cancer cells but can also mediate immunomodulatory effects by reversing KRAS-driven immunosuppressive mechanisms and generate a TME that is more favorable for an anti-tumour immune response (*8, 19, 21*). This knowledge has served as a rationale to investigate clinical combinations of KRAS^{G12C} inhibitors with anti-PD1 or PD-L1 antibodies (*29*). However, previous studies have only validated this combination using mouse models that are highly ICB-responsive (*8, 19*). Here we show that despite the profound TME remodeling caused by KRAS^{G12C} inhibition, this drug combination may not be sufficient to elicit durable responses in tumour models that are intrinsically resistant to immune checkpoint blockade.

Understanding the mechanism of action of KRAS^{G12C} inhibitors and how they can modulate the TME may lead to the identification of additional combination strategies for those patients that will not benefit from the dual inhibition of KRAS^{G12C} and PD-1. Our analysis has gained insight into the different mechanisms by which oncogenic KRAS signaling mediates immune evasion in lung cancer. It has already previously been described that oncogenic KRAS regulates the expression of cytokines and chemokines that can modulate the TME (*22, 30, 31*). Here we show that KRAS^{G12C} inhibition reduces the secretion of monocyte and neutrophil chemoattractants by the tumour cells, which results in an impaired infiltration of these immune suppressive cell types in the TME. Reprograming myeloid populations by targeting selected cytokines or their receptors, like CCR2 (*32*) or CXCR2 (*33*) has been proposed as a mechanism to enhance response to immunotherapies (*34*). Treatment with KRAS^{G12C} inhibitors leads to modulation of various C(X)CL ligands secreted by tumours cells and can thus indirectly reduce immunosuppressive populations without associated toxicities. However, the identity of the KRAS regulated cytokines appears to vary between tumour types.

Another mechanism by which oncogenic KRAS drives immune evasion is by inhibiting IFN responses. We have shown that KRAS^{G12C} inhibitor treatment releases the inhibition of IFN signaling pathway genes in all the models that we have analyzed. Moreover, activation of oncogenic KRAS in type II pneumocytes inhibits IFN pathway expression, suggesting that this is a conserved mechanism in the lung. Mechanistically, KRAS inhibits IFN gene expression via regulation of the oncogene MYC, which is consistent with previous observations in pancreatic cancer (*26*). Importantly, KRAS^{G12C} inhibition enhances tumour cell sensitivity to type I and II interferons and results in an increased IFN pathway activation in vivo. This is especially important as IFN responses are crucial for anti-tumour immunity and clinical responses to

immunotherapies (*23, 24, 35, 36*). By knocking out the IFNγ receptor in tumour cells, we have demonstrated that tumour cell intrinsic IFN signaling is necessary to achieve long-lasting therapeutic responses to KRAS^{G12C} inhibitors in vivo. We have therefore expanded beyond the known role of IFN signaling in the response to immune therapies, showing that an intact interferon response is also required for durable immune responses to a targeted therapy such as KRAS^{G12C} inhibition.

As a consequence of the KRAS-dependent regulation of IFN responses, treatment with KRAS^{G12C} inhibitors increases antigen presentation. Oncogenic KRAS has previously been linked to reduced expression of MHC class I molecules (*37, 38*). Reversion of this immune evasion mechanism can boost T cell recognition rendering tumour cells more susceptible to immune cell attack. Additionally, the cell death induced by KRAS^{G12C} inhibitors could also trigger an adaptive T cell response due to the release of dead cell-associated antigens. Consistent with this, we observe both in vitro and in vivo that KRAS^{G12C} inhibition indirectly increases professional antigen presentation by promoting the activation of APCs accompanied by an increase of CXCR3-binding chemokine expression by DCs. These effects of KRAS^{G12C} inhibition can explain the elevated CD8+ T cell recruitment and the increased T cell activation that we observe upon treatment. Importantly, these characteristics are a prominent feature of 'inflamed' TMEs (*27, 39*), which are more likely to respond to immunotherapy.

KRAS^{G12C} inhibition alleviates immunosuppressive mechanisms and enhances the infiltration and activation of cytotoxic T cells, accompanied by an increase in checkpoint molecule expression, such as PD-1 and LAG-3, even in a very immunosuppressive model like the 3LL ΔNRAS tumours. This TME could be considered optimal for the addition of immune checkpoint blockade inhibitors to potentiate a T-cell dependent immune response (*40*). However, the combination of KRAS^{G12C} inhibition with anti-PD-1 was only synergistic in the immunogenic tumour model (KPAR1.3^{G12C}), but not in the two models that were intrinsically resistant to ICB, one 'cold' tumour model lacking neoantigens (KPB6^{G12C}) and one 'T cell excluded' model which evades anti-tumour immunity by downregulating MHC and recruiting immunosuppressive myeloid cells (3LL ΔNRAS). While we cannot rule out a beneficial effect of the combination in all tumours with immune refractory TMEs, it will be of utmost importance to identify which patients can benefit from the addition of anti-PD-1 inhibitors to KRAS^{G12C} inhibitors and to investigate additional therapeutic strategies for the remaining patients. Our mouse models offer the opportunity for future investigation on additional combinatorial therapies as the therapeutic approach could differ depending on the mechanism of immune evasion. 'Cold' tumour-bearing patients may benefit from the addition of drugs aimed to increase antigen load, such as chemotherapy, radiotherapy, epigenetic modulators or STING agonists (*41*), whereas targeting immunosuppressive cells could be a valid therapeutic strategy

for 'T cell excluded' tumours. KRAS^{G12C} inhibitors can already decrease some myeloid immune suppressive populations, however treatment consistently results in an increase in the infiltration of Tregs, which inhibit cytotoxic T cell activity and might represent an alternative target for combination therapy (*42*).

Several preclinical studies, including this one, have demonstrated that combinations of KRAS^{G12C} inhibitors with immunotherapies can clearly result in therapeutic benefit in immunogenic mouse cancer models (*8, 19*). Based on these data, a number of different clinical trials are underway testing combinations of KRAS^{G12C} inhibitors and PD-1 pathway immune checkpoint blockade, such as KRYSTAL-1, KRYSTAL-7, CodeBreak 100 and CodeBreak 101, with results eagerly awaited. With these and other clinical trials already running, there are still open questions that need to be addressed in order to set up the basis for patient stratification. Our findings are particularly relevant for those patients with highly immune refractory TMEs as they could benefit instead from other combination strategies. While it is likely that the ongoing trials of combinations of KRAS^{G12C} inhibitors with immunotherapies will be beneficial for a subset of KRAS-mutant NSCLC patients, this study has highlighted the need for additional treatment strategies in highly immune refractory patients. In particular, it should be noted that most of these combination clinical trials, with the exception of KRYSTAL-7, do not exclude prior treatment with immunotherapy, and are therefore likely to be enriched with patients whose tumours show either intrinsic or acquired resistance to immune checkpoint blockade. Extrapolating from the preclinical studies reported here, such patients may be less likely to benefit from combinations of KRAS^{G12C} inhibitors with immunotherapies.

While KRAS^{G12C} inhibitors have only recently been approved for clinical use, MEK inhibitors, targeting the MAPK pathway downstream of KRAS, have been used for some time and can result in similar tumour cell-intrinsic immunomodulatory changes (*43*) and in some cases have shown to ameliorate anti-tumour immunity (*44-47*). However, the positive effects in the TME caused by the tumour cell-intrinsic changes can be reduced by the detrimental effects of MEK inhibition on immune cells (*8*). Moreover, although combinations of inhibitors targeting MAPK pathway plus anti-PD-1 can improve clinical outcomes, they do so at the expense of increased toxicities (*48, 49*). In contrast, KRAS^{G12C} inhibitors offer the unique ability to improve anti-tumour immunity via a myriad of mechanisms discussed above while not affecting MAPK signaling in non-tumour cells, including those involved in the anti-tumour immune response. Consequently, unlike other targeted therapies that do not specifically target oncogenic mutant proteins, KRAS^{G12C} inhibitors have the potential to achieve long-term survival which is dependent on the activation of anti-tumour immune responses in immunogenic tumours. The tumour cell-specific activity of KRAS^{G12C} inhibitors provides an unprecedented opportunity to investigate combinations of multiple therapeutic approaches without producing excessive toxicity profiles. Several clinical trials are testing combinations of KRAS^{G12C} inhibitors with other

targeted therapies, including MEK inhibitors (*29*). It will be important to validate that the beneficial effects upon the TME are not lost when these two drug classes are combined. With that in mind, it is possible the “vertical” combinations of $KRAS^{G12C}$ inhibitors with SHP2 inhibitors upstream or CDK4/6 inhibitors downstream may be more promising, as both these drug types have also been shown to produce positive immunomodulatory effects (*20, 50, 51*).

MATERIALS AND METHODS

Study design

The objective of this study was to examine non-tumour cell intrinsic effects of $KRAS^{G12C}$ inhibitors. We performed controlled (non-blinded) laboratory experiments using cancer cell lines to examine the effects of $KRAS^{G12C}$ inhibitors on gene and protein expression and co-culture systems with immune cells to assess indirect effects of the drug treatment on different cell populations. For all in vitro experiments a minimum of two biological replicates (independent experiments) were acquired.

We also used transplantable murine lung cancer models to assess the effects of $KRAS^{G12C}$ inhibitors in non-blinded randomized studies (alone or in combination with ICB) on mouse survival. Endpoints were pre-defined and not modified throughout the duration of the study and mice whose cause of death could not be attributed to lung tumours were excluded. Other in vivo experiments aimed to investigate the TME, by combining RNA, flow cytometry and imaging mass cytometry data. Sample size was chosen empirically based on results of previous studies and no datapoints, including outliers, were excluded from these analyses.

In vivo tumour studies

All studies were performed under a UK Home office approved project license and in accordance with institutional welfare guidelines.

For subcutaneous tumour injection, cells were mixed 1:1 with GeltrexTM matrix (ThermoFisher) and 400,000 3LL ΔNRAS or 150,000 $KPAR^{G12C}$ cells were injected in a total volume of 100μl subcutaneously into one flank of 8-week-old C57BL/6 mice. Tumour growth was followed twice a week by caliper measurements and tumours were left to grow not larger than 1.5cm in diameter following a UK Home Office approved project license.

For orthotopic growth, 10^6 3LL ΔNRAS or 150,000 $KPAR^{G12C}$ cells were injected in PBS in a total volume of 100μl in the tail vein of 8-week-old C57BL/6 mice. Mouse weight was monitored regularly as a measure of tumour growth and mice were sacrificed if weight loss was over 15% as per the UK Home Office approved project license. Tumour burden was also assessed by regular Computed Tomography (CT) scanning of the lungs. Briefly, mice were anesthetized by inhalation of isoflurane and scanned using the Quantum GX2 micro-CT imaging system (Perkin Elmer) at a 50μm isotropic pixel size. Serial lung images were reconstructed and tumour volumes subsequently analyzed using Analyse (AnalyzeDirect).

For therapeutic experiments, mice were treated daily via oral gavage with 50mg/kg MRTX1257 (Mirati Therapeutics), 50mg/kg MRTX849 (MedChemExpress) or 10% Captisol® (Ligand) in 50mM citrate buffer (pH 5.0) as vehicle control.

For ICB treatments, mice were administered 10mg/kg anti-PD-1 (clone RMP1-14, BioXcell), 10mg/kg anti-PD-L1 (clone 10F.9G2, BioXCell) and/or 10mg/kg anti-LAG3 (clone C9B7W, BioXCell) or isotype control (10mg/kg IgG2b and 5mg/kg Syrian hamster IgG2) dissolved in PBS at a dose of 4μl/g mouse intraperitoneally twice a week for a total of four doses.

Statistical analysis

For most experiments, data were compared using unpaired or paired two-tailed Student's t-tests, or ANOVA if more than two experimental groups were examined. In mouse tumour analysis, the Mann-Whitney u-test was used for volume comparison. To compare read counts of individual genes in mRNA-seq datasets of two groups, Wald test was used with a Benjamini and Hochberg correction with an FDR Q value of 5% to obtain adjusted p values (Statistical analysis was performed by Crick Bioinformatics Facility). To compare two survival curves, the Mantel-Cox log-rank test was used. Statistical analyses were performed in Prism 7 (GraphPad Software) or in RStudio. Significance is presented as *P < 0.05, **P < 0.01, ***P < 0.001 and ****P < 0.0001.

SUPPLEMENTARY MATERIALS

Materials and Methods

Fig. S1. KRAS-dependent regulation of secreted factors in human and murine cell lines.

Fig. S2. Mechanism of KRAS-dependent regulation of IFN genes.

Fig. S3. KRAS-driven augmentation of type I and II IFN treatment.

Fig. S4. In vivo characterisation of 3LL ΔNRAS tumours and the effects of $KRAS^{G12C}$ inhibition on myeloid cells.

Fig. S5. $KRAS^{G12C}$ effects on antigen presentation, T cell infiltration and activation in vivo.

Fig. S6. Lack of combinatorial effects of $KRAS^{G12C}$ inhibition and ICB in immune refractory tumours.

Fig. S7. Effects of $KRAS^{G12C}$ inhibition in immunogenic tumours and role of IFN signaling.

References:

1. F. Bray, J. Ferlay, I. Soerjomataram, R. L. Siegel, L. A. Torre, A. Jemal, Global cancer statistics 2018: GLOBOCAN estimates of incidence and mortality worldwide for 36 cancers in 185 countries. *CA Cancer J Clin* **68**, 394-424 (2018).
2. R. L. Siegel, K. D. Miller, A. Jemal, Cancer statistics, 2020. *CA Cancer J Clin* **70**, 7-30 (2020).
3. A. Ribas, J. D. Wolchok, Cancer immunotherapy using checkpoint blockade. *Science* **359**, 1350-1355 (2018).
4. P. Sharma, S. Hu-Lieskovan, J. A. Wargo, A. Ribas, Primary, Adaptive, and Acquired Resistance to Cancer Immunotherapy. *Cell* **168**, 707-723 (2017).
5. W. Pao, K. E. Hutchinson, Chipping away at the lung cancer genome. *Nat Med* **18**, 349-351 (2012).
6. A. P. G. Consortium, AACR Project GENIE: Powering Precision Medicine through an International Consortium. *Cancer Discov* **7**, 818-831 (2017).
7. J. M. Ostrem, U. Peters, M. L. Sos, J. A. Wells, K. M. Shokat, K-Ras(G12C) inhibitors allosterically control GTP affinity and effector interactions. *Nature* **503**, 548-551 (2013).
8. J. Canon, K. Rex, A. Y. Saiki, C. Mohr, K. Cooke, D. Bagal, K. Gaida, T. Holt, C. G. Knutson, N. Koppada, B. A. Lanman, J. Werner, A. S. Rapaport, T. San Miguel, R. Ortiz, T. Osgood, J. R. Sun, X. Zhu, J. D. McCarter, L. P. Volak, B. E. Houk, M. G. Fakih, B. H. O'Neil, T. J. Price, G. S. Falchook, J. Desai, J. Kuo, R. Govindan, D. S. Hong, W. Ouyang, H. Henary, T. Arvedson, V. J. Cee, J. R. Lipford, The clinical KRAS(G12C) inhibitor AMG 510 drives anti-tumour immunity. *Nature* **575**, 217-223 (2019).
9. D. S. Hong, M. G. Fakih, J. H. Strickler, J. Desai, G. A. Durm, G. I. Shapiro, G. S. Falchook, T. J. Price, A. Sacher, C. S. Denlinger, Y. J. Bang, G. K. Dy, J. C. Krauss, Y. Kuboki, J. C. Kuo, A. L. Coveler, K. Park, T. W. Kim, F. Barlesi, P. N. Munster, S. S. Ramalingam, T. F. Burns, F. Meric-Bernstam, H. Henary, J. Ngang, G. Ngarmchamnanrith, J. Kim, B. E. Houk, J. Canon, J. R. Lipford, G. Friberg, P. Lito, R. Govindan, B. T. Li, KRAS(G12C) Inhibition with Sotorasib in Advanced Solid Tumors. *N Engl J Med* **383**, 1207-1217 (2020).
10. F. Skoulidis, B. T. Li, G. K. Dy, T. J. Price, G. S. Falchook, J. Wolf, A. Italiano, M. Schuler, H. Borghaei, F. Barlesi, T. Kato, A. Curioni-Fontecedro, A. Sacher, A. Spira, S. S. Ramalingam, T. Takahashi, B. Besse, A. Anderson, A. Ang, Q. Tran, O. Mather, H. Henary, G. Ngarmchamnanrith, G. Friberg, V. Velcheti, R. Govindan, Sotorasib for Lung Cancers with KRAS p.G12C Mutation. *N Engl J Med* **384**, 2371-2381 (2021).

11. N. Tanaka, J. J. Lin, C. Li, M. B. Ryan, J. Zhang, L. A. Kiedrowski, A. G. Michel, M. U. Syed, K. A. Fella, M. Sakhi, I. Baiev, D. Juric, J. F. Gainor, S. J. Klempner, J. K. Lennerz, G. Siravegna, L. Bar-Peled, A. N. Hata, R. S. Heist, R. B. Corcoran, Clinical Acquired Resistance to KRAS(G12C) Inhibition through a Novel KRAS Switch-II Pocket Mutation and Polyclonal Alterations Converging on RAS-MAPK Reactivation. *Cancer Discov* **11**, 1913-1922 (2021).
12. M. M. Awad, S. Liu, Rybkin, II, K. C. Arbour, J. Dilly, V. W. Zhu, M. L. Johnson, R. S. Heist, T. Patil, G. J. Riely, J. O. Jacobson, X. Yang, N. S. Persky, D. E. Root, K. E. Lowder, H. Feng, S. S. Zhang, K. M. Haigis, Y. P. Hung, L. M. Sholl, B. M. Wolpin, J. Wiese, J. Christiansen, J. Lee, A. B. Schrock, L. P. Lim, K. Garg, M. Li, L. D. Engstrom, L. Waters, J. D. Lawson, P. Olson, P. Lito, S. I. Ou, J. G. Christensen, P. A. Janne, A. J. Aguirre, Acquired Resistance to KRAS(G12C) Inhibition in Cancer. *N Engl J Med* **384**, 2382-2393 (2021).
13. T. Koga, K. Suda, T. Fujino, S. Ohara, A. Hamada, M. Nishino, M. Chiba, M. Shimoji, T. Takemoto, T. Arita, M. Gmachl, M. H. Hofmann, J. Soh, T. Mitsudomi, KRAS Secondary Mutations That Confer Acquired Resistance to KRAS G12C Inhibitors, Sotorasib and Adagrasib, and Overcoming Strategies: Insights From In Vitro Experiments. *J Thorac Oncol* **16**, 1321-1332 (2021).
14. M. Molina-Arcas, C. Moore, S. Rana, F. van Maldegem, E. Mugarza, P. Romero-Clavijo, E. Herbert, S. Horswell, L. S. Li, M. R. Janes, D. C. Hancock, J. Downward, Development of combination therapies to maximize the impact of KRAS-G12C inhibitors in lung cancer. *Sci Transl Med* **11**, (2019).
15. V. Dunnett-Kane, P. Nicola, F. Blackhall, C. Lindsay, Mechanisms of Resistance to KRAS(G12C) Inhibitors. *Cancers (Basel)* **13**, (2021).
16. N. A. Rizvi, M. D. Hellmann, A. Snyder, P. Kvistborg, V. Makarov, J. J. Havel, W. Lee, J. Yuan, P. Wong, T. S. Ho, M. L. Miller, N. Rekhtman, A. L. Moreira, F. Ibrahim, C. Bruggeman, B. Gasmi, R. Zappasodi, Y. Maeda, C. Sander, E. B. Garon, T. Merghoub, J. D. Wolchok, T. N. Schumacher, T. A. Chan, Cancer immunology. Mutational landscape determines sensitivity to PD-1 blockade in non-small cell lung cancer. *Science* **348**, 124-128 (2015).
17. P. Martinez, S. Peters, T. Stammers, J. C. Soria, Immunotherapy for the First-Line Treatment of Patients with Metastatic Non-Small Cell Lung Cancer. *Clin Cancer Res* **25**, 2691-2698 (2019).
18. J. Cullis, S. Das, D. Bar-Sagi, Kras and Tumor Immunity: Friend or Foe? *Cold Spring Harb Perspect Med* **8**, (2018).
19. D. M. Briere, S. Li, A. Calinisan, N. Sudhakar, R. Aranda, L. Hargis, D. H. Peng, J. Deng, L. D. Engstrom, J. Hallin, S. Gatto, J. Fernandez-Banet, A. Pavlicek, K. K. Wong,

J. G. Christensen, P. Olson, The KRAS(G12C) Inhibitor MRTX849 Reconditions the Tumor Immune Microenvironment and Sensitizes Tumors to Checkpoint Inhibitor Therapy. *Mol Cancer Ther* **20**, 975-985 (2021).

20. C. Fedele, S. Li, K. W. Teng, C. J. R. Foster, D. Peng, H. Ran, P. Mita, M. J. Geer, T. Hattori, A. Koide, Y. Wang, K. H. Tang, J. Leinwand, W. Wang, B. Diskin, J. Deng, T. Chen, I. Dolgalev, U. Ozerdem, G. Miller, S. Koide, K. K. Wong, B. G. Neel, SHP2 inhibition diminishes KRASG12C cycling and promotes tumor microenvironment remodeling. *J Exp Med* **218**, (2021).
21. F. van Maldegem, K. Valand, M. Cole, H. Patel, M. Angelova, S. Rana, E. Colliver, K. Enfield, N. Bah, V. S. K. Tsang, E. Mugarza, C. Moore, P. Hobson, D. Levi, M. Molina-Arcas, C. Swanton, J. Downward, Characterisation of tumour immune microenvironment remodelling following oncogene inhibition in preclinical studies using an optimised imaging mass cytometry workflow. *bioRxiv*, 2021.2002.2002.429358 (2021).
22. Y. Pylayeva-Gupta, K. E. Lee, C. H. Hajdu, G. Miller, D. Bar-Sagi, Oncogenic Kras-induced GM-CSF production promotes the development of pancreatic neoplasia. *Cancer Cell* **21**, 836-847 (2012).
23. D. H. Kaplan, V. Shankaran, A. S. Dighe, E. Stockert, M. Aguet, L. J. Old, R. D. Schreiber, Demonstration of an interferon gamma-dependent tumor surveillance system in immunocompetent mice. *Proc Natl Acad Sci U S A* **95**, 7556-7561 (1998).
24. J. M. Zaretsky, A. Garcia-Diaz, D. S. Shin, H. Escuin-Ordinas, W. Hugo, S. Hu-Lieskovan, D. Y. Torrejon, G. Abril-Rodriguez, S. Sandoval, L. Barthly, J. Saco, B. Homet Moreno, R. Mezzadra, B. Chmielowski, K. Ruchalski, I. P. Shintaku, P. J. Sanchez, C. Puig-Saus, G. Cherry, E. Seja, X. Kong, J. Pang, B. Berent-Maoz, B. Comin-Anduix, T. G. Graeber, P. C. Tumeh, T. N. Schumacher, R. S. Lo, A. Ribas, Mutations Associated with Acquired Resistance to PD-1 Blockade in Melanoma. *N Engl J Med* **375**, 819-829 (2016).
25. S. de Carné Trécesson, J. Boumelha, E. K. Law, P. Romero-Clavijo, E. Mugarza, M. A. Coelho, C. Moore, S. Rana, D. R. Caswell, M. Murillo, D. C. Hancock, P. P. Argyris, W. L. Brown, C. Durfee, L. K. Larson, R. I. Vogel, A. Suárez-Bonnet, S. L. Priestnall, P. East, S. J. Ross, M. Molina-Arcas, C. Swanton, R. Harris, J. Downward, APOBEC3B expression generates an immunogenic model of Kras mutant lung cancer. *bioRxiv*, 2020.2012.2022.423126 (2020).
26. N. Muthalagu, T. Monteverde, X. Raffo-Iraolagoitia, R. Wiesheu, D. Whyte, A. Hedley, S. Laing, B. Kruspig, R. Upstill-Goddard, R. Shaw, S. Neidler, C. Rink, S. A. Karim, K. Gyuraszova, C. Nixon, W. Clark, A. V. Biankin, L. M. Carlin, S. B. Coffelt, O. J. Sansom, J. P. Morton, D. J. Murphy, Repression of the Type I Interferon Pathway Underlies

MYC- and KRAS-Dependent Evasion of NK and B Cells in Pancreatic Ductal Adenocarcinoma. *Cancer Discov* **10**, 872-887 (2020).

27. S. Spranger, D. Dai, B. Horton, T. F. Gajewski, Tumor-Residing Batf3 Dendritic Cells Are Required for Effector T Cell Trafficking and Adoptive T Cell Therapy. *Cancer Cell* **31**, 711-723 e714 (2017).
28. S. Li, Y. Simoni, S. Zhuang, A. Gabel, S. Ma, J. Chee, L. Islas, A. Cessna, J. Creaney, R. K. Bradley, A. Redwood, B. W. Robinson, E. W. Newell, Characterization of neoantigen-specific T cells in cancer resistant to immune checkpoint therapies. *Proc Natl Acad Sci U S A* **118**, (2021).
29. M. Molina-Arcas, A. Samani, J. Downward, Drugging the Undruggable: Advances on RAS Targeting in Cancer. *Genes (Basel)* **12**, (2021).
30. H. Ji, A. M. Houghton, T. J. Mariani, S. Perera, C. B. Kim, R. Padera, G. Tonon, K. McNamara, L. A. Marconcini, A. Hezel, N. El-Bardeesy, R. T. Bronson, D. Sugarbaker, R. S. Maser, S. D. Shapiro, K. K. Wong, K-ras activation generates an inflammatory response in lung tumors. *Oncogene* **25**, 2105-2112 (2006).
31. S. Hamarsheh, O. Gross, T. Brummer, R. Zeiser, Immune modulatory effects of oncogenic KRAS in cancer. *Nat Commun* **11**, 5439 (2020).
32. T. M. Nywening, A. Wang-Gillam, D. E. Sanford, B. A. Belt, R. Z. Panni, B. M. Cusworth, A. T. Toriola, R. K. Nieman, L. A. Worley, M. Yano, K. J. Fowler, A. C. Lockhart, R. Suresh, B. R. Tan, K. H. Lim, R. C. Fields, S. M. Strasberg, W. G. Hawkins, D. G. DeNardo, S. P. Goedegebuure, D. C. Linehan, Targeting tumour-associated macrophages with CCR2 inhibition in combination with FOLFIRINOX in patients with borderline resectable and locally advanced pancreatic cancer: a single-centre, open-label, dose-finding, non-randomised, phase 1b trial. *Lancet Oncol* **17**, 651-662 (2016).
33. C. W. Steele, S. A. Karim, J. D. G. Leach, P. Bailey, R. Upstill-Goddard, L. Rishi, M. Foth, S. Bryson, K. McDaid, Z. Wilson, C. Eberlein, J. B. Candido, M. Clarke, C. Nixon, J. Connelly, N. Jamieson, C. R. Carter, F. Balkwill, D. K. Chang, T. R. J. Evans, D. Strathdee, A. V. Biankin, R. J. B. Nibbs, S. T. Barry, O. J. Sansom, J. P. Morton, CXCR2 Inhibition Profoundly Suppresses Metastases and Augments Immunotherapy in Pancreatic Ductal Adenocarcinoma. *Cancer Cell* **29**, 832-845 (2016).
34. Y. Zhu, W. G. Hawkins, D. G. DeNardo, Regramming myeloid responses to improve cancer immunotherapy. *Oncoimmunology* **4**, e974399 (2015).
35. A. S. Dighe, E. Richards, L. J. Old, R. D. Schreiber, Enhanced in vivo growth and resistance to rejection of tumor cells expressing dominant negative IFN gamma receptors. *Immunity* **1**, 447-456 (1994).

36. J. Gao, L. Z. Shi, H. Zhao, J. Chen, L. Xiong, Q. He, T. Chen, J. Roszik, C. Bernatchez, S. E. Woodman, P. L. Chen, P. Hwu, J. P. Allison, A. Futreal, J. A. Wargo, P. Sharma, Loss of IFN-gamma Pathway Genes in Tumor Cells as a Mechanism of Resistance to Anti-CTLA-4 Therapy. *Cell* **167**, 397-404 e399 (2016).
37. B. Seliger, C. Harders, U. Wollscheid, M. S. Staege, A. B. Reske-Kunz, C. Huber, Suppression of MHC class I antigens in oncogenic transformants: association with decreased recognition by cytotoxic T lymphocytes. *Exp Hematol* **24**, 1275-1279 (1996).
38. D. Atkins, A. Breuckmann, G. E. Schmahl, P. Binner, S. Ferrone, F. Krummenauer, S. Storkel, B. Seliger, MHC class I antigen processing pathway defects, ras mutations and disease stage in colorectal carcinoma. *Int J Cancer* **109**, 265-273 (2004).
39. H. Harlin, Y. Meng, A. C. Peterson, Y. Zha, M. Tretiakova, C. Slingluff, M. McKee, T. F. Gajewski, Chemokine expression in melanoma metastases associated with CD8+ T-cell recruitment. *Cancer Res* **69**, 3077-3085 (2009).
40. J. Galon, D. Bruni, Approaches to treat immune hot, altered and cold tumours with combination immunotherapies. *Nat Rev Drug Discov* **18**, 197-218 (2019).
41. P. Gotwals, S. Cameron, D. Cipolletta, V. Cremasco, A. Crystal, B. Hewes, B. Mueller, S. Quaratino, C. Sabatos-Peyton, L. Petruzzelli, J. A. Engelman, G. Dranoff, Prospects for combining targeted and conventional cancer therapy with immunotherapy. *Nat Rev Cancer* **17**, 286-301 (2017).
42. F. Arce Vargas, A. J. S. Furness, K. Litchfield, K. Joshi, R. Rosenthal, E. Ghorani, I. Solomon, M. H. Lesko, N. Ruef, C. Roddie, J. Y. Henry, L. Spain, A. Ben Aissa, A. Georgiou, Y. N. S. Wong, M. Smith, D. Strauss, A. Hayes, D. Nicol, T. O'Brien, L. Martensson, A. Ljungars, I. Teige, B. Frendeus, T. R. Melanoma, T. R. Renal, T. R. L. consortia, M. Pule, T. Marafioti, M. Gore, J. Larkin, S. Turajlic, C. Swanton, K. S. Peggs, S. A. Quezada, Fc Effector Function Contributes to the Activity of Human Anti-CTLA-4 Antibodies. *Cancer Cell* **33**, 649-663 e644 (2018).
43. S. Hu-Lieskovan, S. Mok, B. Homet Moreno, J. Tsoi, L. Robert, L. Goedert, E. M. Pinheiro, R. C. Koya, T. G. Graeber, B. Comin-Anduix, A. Ribas, Improved antitumor activity of immunotherapy with BRAF and MEK inhibitors in BRAF(V600E) melanoma. *Sci Transl Med* **7**, 279ra241 (2015).
44. P. J. R. Ebert, J. Cheung, Y. Yang, E. McNamara, R. Hong, M. Moskalenko, S. E. Gould, H. Maecker, B. A. Irving, J. M. Kim, M. Belvin, I. Mellman, MAP Kinase Inhibition Promotes T Cell and Anti-tumor Activity in Combination with PD-L1 Checkpoint Blockade. *Immunity* **44**, 609-621 (2016).
45. H. Choi, J. Deng, S. Li, T. Silk, L. Dong, E. J. Brea, S. Houghton, D. Redmond, H. Zhong, J. Boiarsky, E. A. Akbay, P. D. Smith, T. Merghoub, K. K. Wong, J. D. Wolchok,

Pulsatile MEK Inhibition Improves Anti-tumor Immunity and T Cell Function in Murine Kras Mutant Lung Cancer. *Cell Rep* **27**, 806-819 e805 (2019).

46. S. Loi, S. Dushyanthen, P. A. Beavis, R. Salgado, C. Denkert, P. Savas, S. Combs, D. L. Rimm, J. M. Giltnane, M. V. Estrada, V. Sanchez, M. E. Sanders, R. S. Cook, M. A. Pilkinton, S. A. Mallal, K. Wang, V. A. Miller, P. J. Stephens, R. Yelensky, F. D. Doimi, H. Gomez, S. V. Ryzhov, P. K. Darcy, C. L. Arteaga, J. M. Balko, RAS/MAPK Activation Is Associated with Reduced Tumor-Infiltrating Lymphocytes in Triple-Negative Breast Cancer: Therapeutic Cooperation Between MEK and PD-1/PD-L1 Immune Checkpoint Inhibitors. *Clin Cancer Res* **22**, 1499-1509 (2016).
47. S. M. Reddy, A. Reuben, J. A. Wargo, Influences of BRAF Inhibitors on the Immune Microenvironment and the Rationale for Combined Molecular and Immune Targeted Therapy. *Curr Oncol Rep* **18**, 42 (2016).
48. A. Ribas, D. Lawrence, V. Atkinson, S. Agarwal, W. H. Miller, Jr., M. S. Carlino, R. Fisher, G. V. Long, F. S. Hodi, J. Tsoi, C. S. Grasso, B. Mookerjee, Q. Zhao, R. Ghori, B. H. Moreno, N. Ibrahim, O. Hamid, Combined BRAF and MEK inhibition with PD-1 blockade immunotherapy in BRAF-mutant melanoma. *Nat Med* **25**, 936-940 (2019).
49. R. Gutzmer, D. Stroyakovskiy, H. Gogas, C. Robert, K. Lewis, S. Protsenko, R. P. Pereira, T. Eigentler, P. Rutkowski, L. Demidov, G. M. Manikhas, Y. Yan, K. C. Huang, A. Uyei, V. McNally, G. A. McArthur, P. A. Ascierto, Atezolizumab, vemurafenib, and cobimetinib as first-line treatment for unresectable advanced BRAF(V600) mutation-positive melanoma (IMspire150): primary analysis of the randomised, double-blind, placebo-controlled, phase 3 trial. *Lancet* **395**, 1835-1844 (2020).
50. E. Quintana, C. J. Schulze, D. R. Myers, T. J. Choy, K. Mordec, D. Wildes, N. T. Shifrin, A. Belwafa, E. S. Koltun, A. L. Gill, M. Singh, S. Kelsey, M. A. Goldsmith, R. Nichols, J. A. M. Smith, Allosteric Inhibition of SHP2 Stimulates Antitumor Immunity by Transforming the Immunosuppressive Environment. *Cancer Res* **80**, 2889-2902 (2020).
51. J. Deng, E. S. Wang, R. W. Jenkins, S. Li, R. Dries, K. Yates, S. Chhabra, W. Huang, H. Liu, A. R. Aref, E. Ivanova, C. P. Paweletz, M. Bowden, C. W. Zhou, G. S. Herter-Sprie, J. A. Sorrentino, J. E. Bisi, P. H. Lizotte, A. A. Merlino, M. M. Quinn, L. E. Bufe, A. Yang, Y. Zhang, H. Zhang, P. Gao, T. Chen, M. E. Cavanaugh, A. J. Rode, E. Haines, P. J. Roberts, J. C. Strum, W. G. Richards, J. H. Lorch, S. Parangi, V. Gunda, G. M. Boland, R. Bueno, S. Palakurthi, G. J. Freeman, J. Ritz, W. N. Haining, N. E. Sharpless, H. Arthanari, G. I. Shapiro, D. A. Barbie, N. S. Gray, K. K. Wong, CDK4/6 Inhibition Augments Antitumor Immunity by Enhancing T-cell Activation. *Cancer Discov* **8**, 216-233 (2018).

Acknowledgments:

We thank the science technology platforms at the Francis Crick Institute including the Biological Research Facility, Advanced Sequencing Facility, Computational Biology, Genomics Equipment Park, Experimental Histopathology, FACS and Cell Services. We thank Philip Hobson and Dina Levi for assistance with imaging mass cytometry. **Funding:** This work was supported by the Francis Crick Institute, which receives its core funding from Cancer Research UK (FC001070), the UK Medical Research Council (FC001070), and the Wellcome Trust (FC001070), and by funding to JD from the European Research Council Advanced Grant RASIMMUNE and a Wellcome Trust Senior Investigator Award 103799/Z/14/Z. **Author Contributions**: E.M, F.vM., M.M-A., and J.D. designed the study, interpreted the results and wrote the manuscript. E.M, F.vM, M.M-A., S.R., J.B., R.A., P.A., P.R.C., K.V. performed the biochemical experiments, C.M. assisted with *in vivo* studies, M.L.S. and P.E. performed bioinformatics analyses. All authors contributed to manuscript revision and review. **Competing interests:** J.D. has acted as a consultant for AstraZeneca, Bayer, Jubilant, Theras, BridgeBio, Vividion and Novartis, and has funded research agreements with BMS and Revolution Medicines. None of the other authors of this manuscript have a financial interest related to this work. **Data and materials availability:** RNA sequencing data has been deposited at Gene Expression Omnibus (accession code GSE183549).

Figure 1

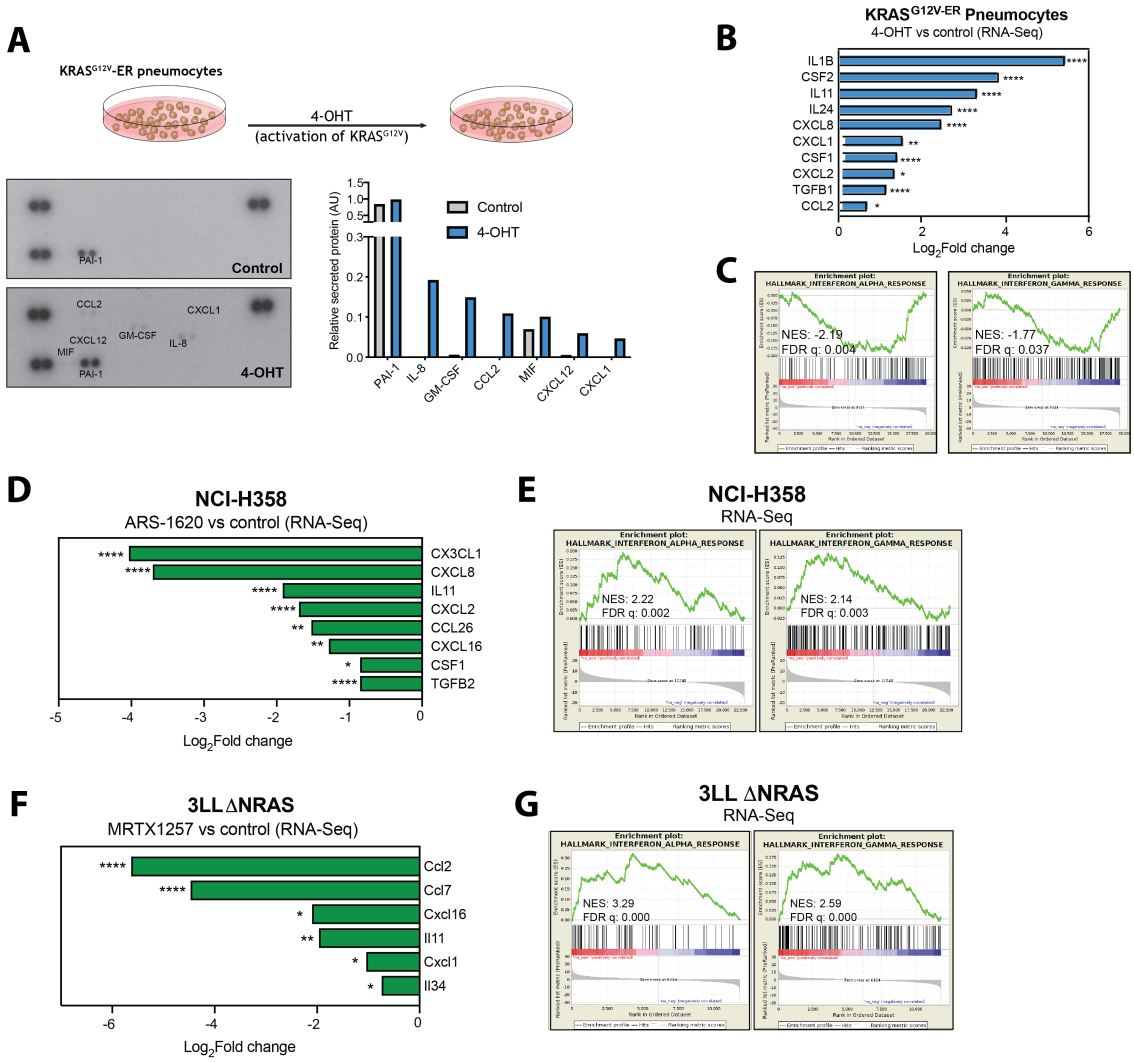

Fig. 1. Oncogenic KRAS regulates immune gene expression in cell lines. (A) Cytokine array of cell culture supernatant from KRAS$^{G12V-ER}$ pneumocytes treated with 500nM 4-OHT or ethanol control for 24h. Graph shows secreted protein relative to control spots on the array for each condition. (B) Log_2Fold change of selected cytokine genes from RNA-Seq data in 4-OHT (500nM, 24h treated KRAS$^{G12V-ER}$ pneumocytes. (C) MSigDB Hallmarks gene set enrichment analysis (GSEA) plots of IFNα and IFNγ pathways in 4-OHT treated versus control samples. (D) Log_2Fold change of selected cytokine genes from RNA-Seq data in ARS-1620 (2μM, 24h) treated NCI-H358 cells versus DMSO control. (E) MSigDB Hallmarks GSEA plots of IFNα and IFNγ pathways in ARS-1620 treated versus control samples. (F) Same analysis as (D) of RNA-Seq from 3LL ΔNRAS cells treated with 100nM MRTX1257 (24h, n=3). (G) Same analysis as (E) of RNA-Seq from 3LL ΔNRAS cells. All statistics represent FDR adjusted p values (q<0.05).

Figure 2

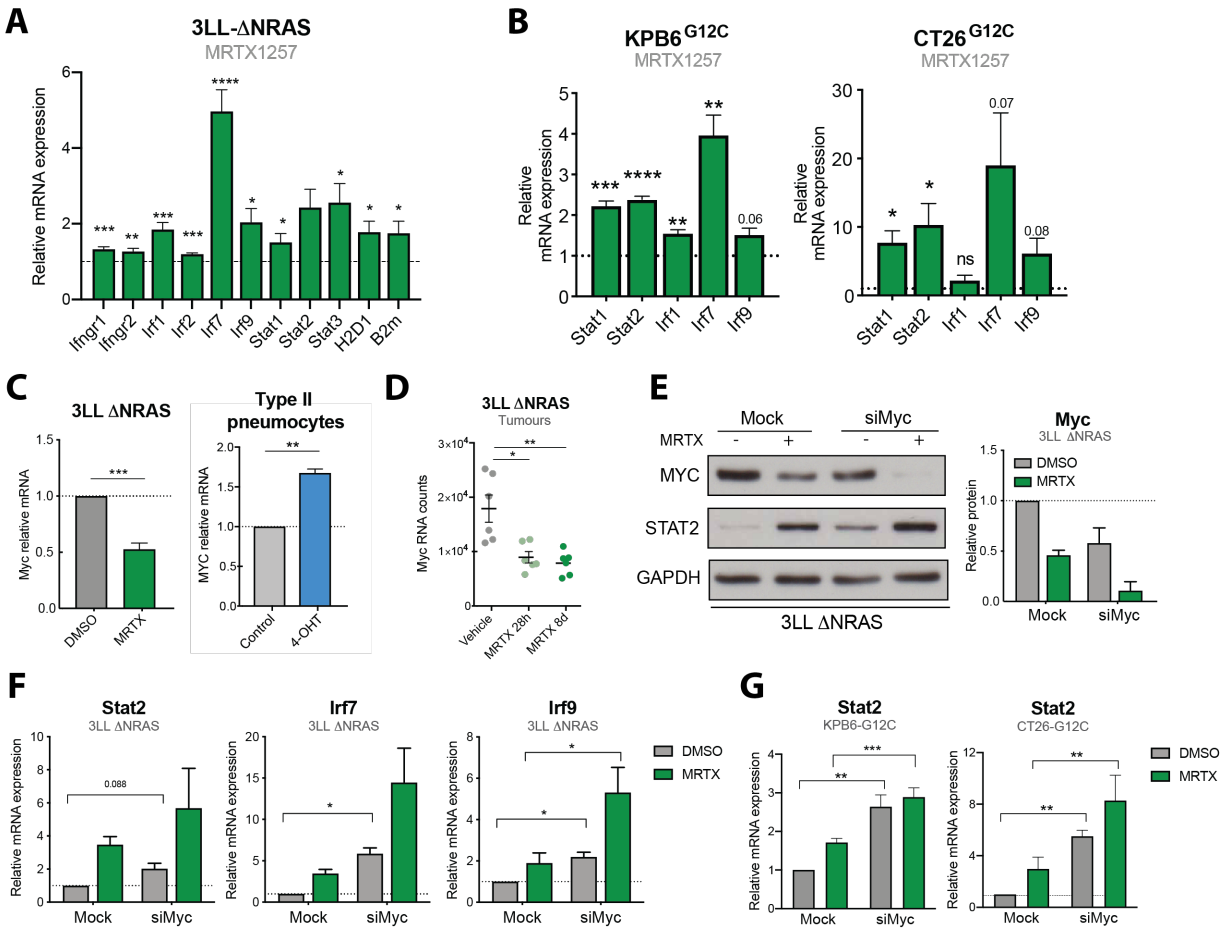

Fig. 2. KRAS signaling downregulates IFN pathway gene expression via MYC. (A) qPCR analysis of IFN-induced genes in MRTX1257-treated (100nM, 24h) 3LL ΔNRAS cells ($2^{-\Delta\Delta CT}$, normalised to control sample for all genes, n=6, unpaired t test, mean+SEM). (B) Same as (A) using KPB6^{G12C} (n=4) and CT26^{G12C} (n=3) cell lines. (C) qPCR showing KRAS-dependent regulation of Myc in 3LL ΔNRAS cells (n=3) after treatment with MRTX and KRAS$^{G12V\text{-}ER}$ pneumocytes (n=4) after treatment with 4-OHT (unpaired t test, mean+SEM). (D) RNA-Seq mRNA counts of 3LL ΔNRAS lung tumours treated with vehicle or 50mg/kg MRTX1257 for 28h or 8 days (each dot represents a tumour, n=6 per group, FDR p adjusted value). (E) Western blot showing MYC knockdown and STAT2 upregulation of 3LL ΔNRAS cells treated with 100nM MRTX (24h), Myc siRNA (48h), or both. Quantification for two independent experiments is shown on the right (mean+SEM). (F) qPCR analysis of IFN-induced genes in 3LL ΔNRAS cells treated with MRTX, Myc siRNA or both ($2^{-\Delta\Delta CT}$, normalised to control sample for all genes, n=3, paired t tests siMyc versus Mock, mean+SEM). (G) Same analysis as (F) in KPB6^{G12C} (n=4) and CT26^{G12C} (n=3) cells.

Figure 3

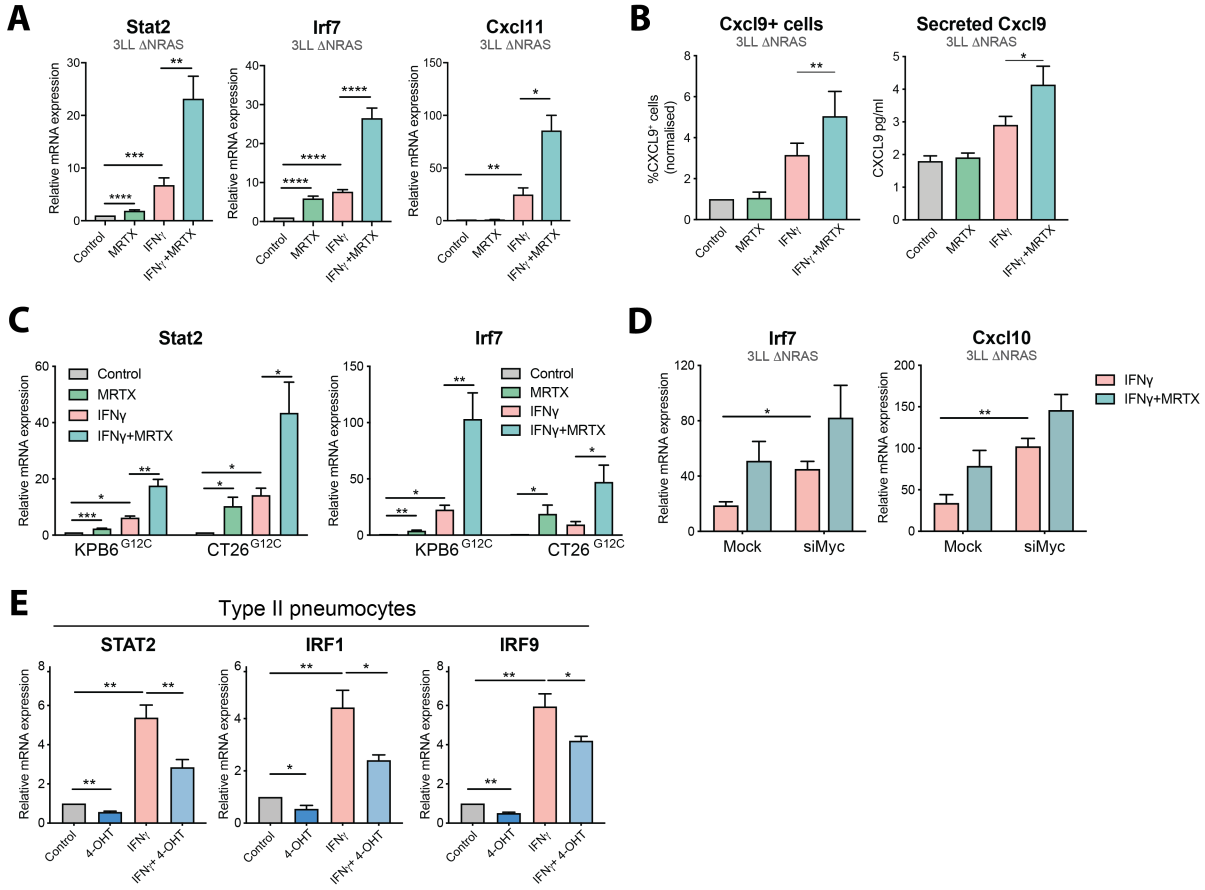

Fig. 3. KRAS^{G12C} inhibition enhances tumour cell intrinsic IFN responses. (A) qPCR analysis of IFN-induced genes in MRTX1257 (100nM, 24h) and/or recombinant IFNγ (100ng/ml) treated 3LL ΔNRAS cells ($2^{-\Delta\Delta CT}$, normalised to control sample for all genes, n=6, paired t test, mean+SEM). (B) Protein validation of IFN response regulation by KRAS. Left: Percentage of CXCL9-positive cells as measured by flow cytometry on 3LL ΔNRAS cells after treatment with MRTX and/or IFNγ. Right: concentration of CXCL9 secreted to the medium of 3LL ΔNRAS cells after treatment with MRTX and/or IFNγ, measured by ELISA (normalised to control sample, n=3, paired t test, mean+SEM for both). (C) Same as (A) using KPB6^{G12C} (n=4) and CT26^{G12C} (n=3) cell lines. (D) qPCR analysis of IFN-induced genes in 3LL ΔNRAS cells treated with IFNγ only or IFNγ and MRTX in presence of 48h of Mock or Myc siRNA ($2^{-\Delta\Delta CT}$, normalised to IFNγ only-treated sample for all genes, n=3, paired t test, mean+SEM). (E) qPCR analysis of IFN pathway genes in human KRAS$^{G12V\text{-}ER}$ pneumocytes after treatment with 4-OHT and/or recombinant IFNγ for 24h (normalised to control sample n=4, paired t test, mean+SEM).

Figure 4

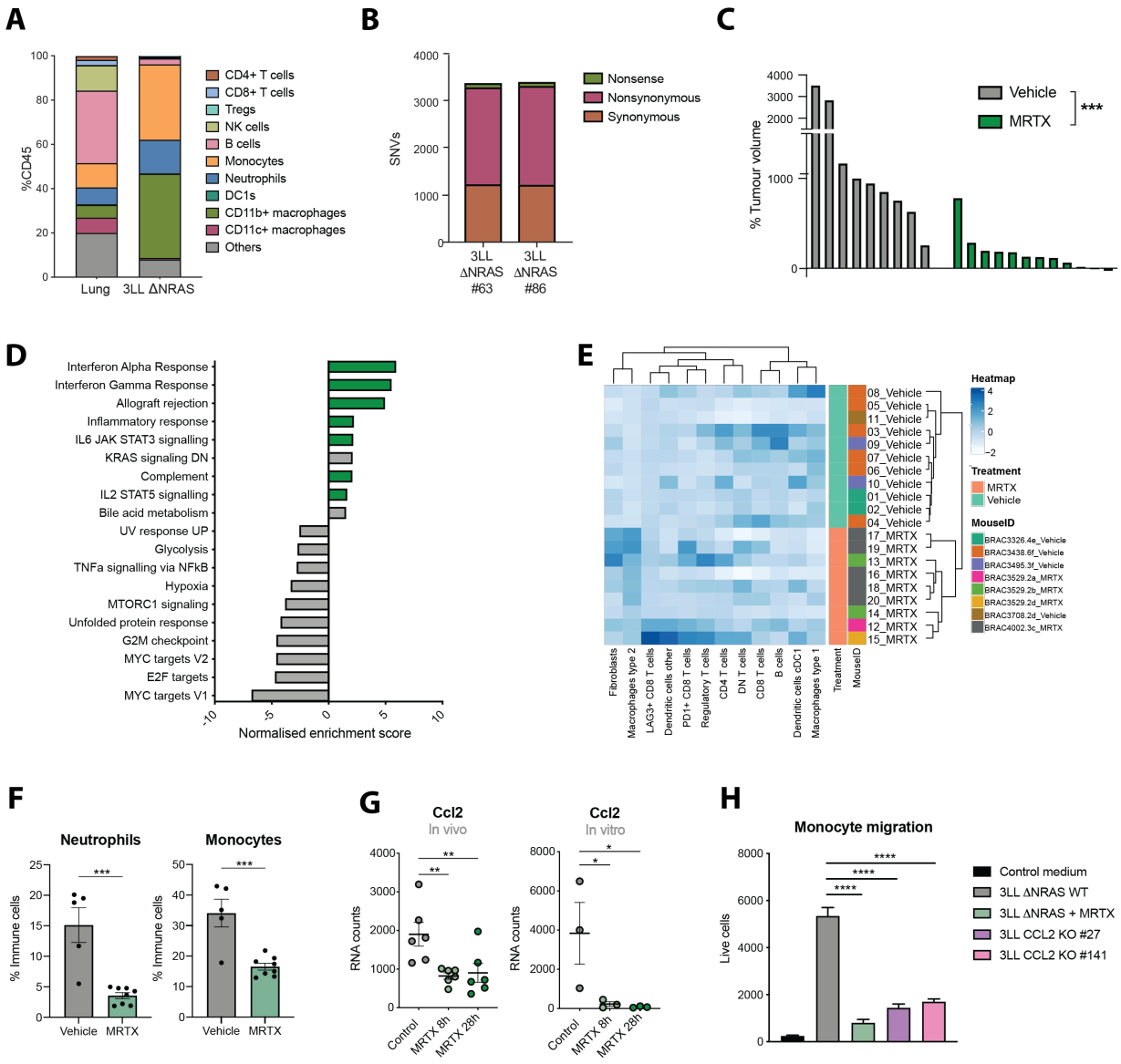

Fig. 4. KRAS^{G12C} inhibition remodels the immunosuppressive TME of 3LL ΔNRAS lung tumours. (A) Immunophenotyping of dissected lung tumours obtained by intravenous administration of 3LL ΔNRAS cells (n=5 mice) versus healthy lung tissue (n=6 mice) obtained by flow cytometry. (B) Whole exome sequencing SNV analysis of two NRAS CRISPR-edited 3LL clones. (C) Post-treatment tumour volume change as measured by μCT scanning of 3LL ΔNRAS lung tumours after one week of treatment with vehicle control or 50mg/kg MRTX1257 (Each bar represents one tumour, Mann-Whitney test). (D) Summary of significantly (FDR q<0.05) up- and down-regulated pathways in MRTX- versus vehicle-treated lung tumours (MSigDB Hallmarks). (E) Hierarchical clustering of relative frequencies of tumour infiltrating cell types in MRTX- and vehicle-treated tumours obtained by IMC. (F) Percentage of neutrophils

(gated as CD45+ CD11b+ Ly6C+ Ly6G+) and monocytes (gated as CD45+ CD11b+ Ly6C^{hi} Ly6G-) in vehicle (n=5) and MRTX-treated (n=8) lung tumours measured by flow cytometry (each dot represents a mouse, unpaired t test). (G) mRNA counts for *Ccl2* gene in MRTX treated 3LL ΔNRAS tumours (n=6 per group, left) and cells (n=3, right) obtained by RNA-Seq (FDR adjusted p value). H) Live cell count (by flow cytometry) of bone marrow-derived monocytes that have migrated through a transwell in presence of conditioned medium from 3LL ΔNRAS cells, MRTX-treated cells or two clones from *Ccl2* CRISPR knockout (n=3 independent experiments, one-way ANOVA).

Figure 5

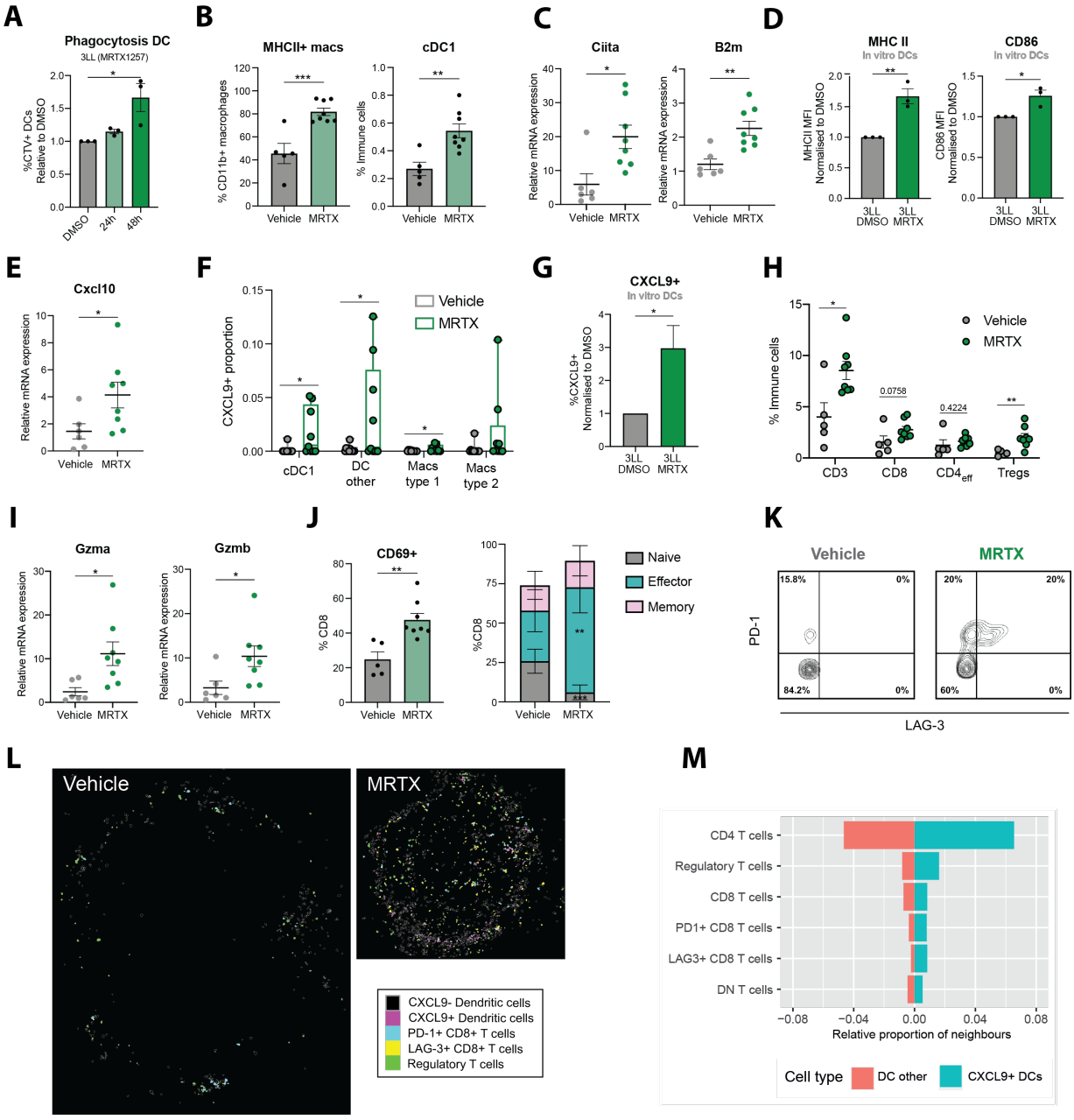

Fig. 5. KRAS^{G12C} inhibition promotes professional antigen presentation, T cell infiltration and activation. (A) Normalised percentage of GFP+ Mutu dendritic cells that have phagocytosed CTV+ 3LL ΔNRAS cells, previously treated with DMSO control, or 100nM MRTX1257 for 24h or 48h, measured by flow cytometry (n=3 independent experiments, One-way ANOVA, mean±SEM). (B) Flow cytometry analysis of 3LL ΔNRAS lung tumours treated with vehicle or 50mg/kg MRTX1257 for 7 days. Macrophages are gated as Live CD45+ CD11b+ CD24- CD64+ and DC1s are obtained by Live, CD45+, CD11c+ CD24+ CD103+ gating (n=5 for vehicle n=8 mice for MRTX-treated, unpaired t test, mean±SEM). (C) qPCR data for 3LL ΔNRAS lung tumours treated as in (B) ($2^{-\Delta\Delta CT}$, unpaired t test, n=7 vehicle, n=8

treated, mean±SEM). (D) Normalised mean fluorescence intensity of MHCII and CD86 as measured by flow cytometry of DCs co-cultured with 3LL ΔNRAS cells previously treated with either DMSO or MRTX for 48h (pre-gated as GFP+, unpaired t test, n=3 independent experiments, mean±SEM). (E) qPCR data of Cxcl10 gene in 3LL ΔNRAS tumours, analyzed as in (C). (F) Proportion of CXCL9+ cells in each population, as detected by IMC, per ROI (n=11 vehicle, n=9 MRTX, unpaired t tests, mean±SEM). (G) Normalised percentage of CXCL9+ DCs after co-culture with 3LL ΔNRAS cells as in (D) (n=5 independent experiments, unpaired t test, mean+SEM). (H) Summary of T cell infiltration measured by flow cytometry in vehicle versus MRTX-treated lung tumours (n=5 for vehicle, n=8 mice for treated, unpaired t tests). (I) qPCR analysis of cytotoxicity genes in 3LL ΔNRAS lung tumours, analyzed as in (C). (J) Flow cytometry analysis of CD8+ T cell phenotypes. Left: percentage of CD69+ CD8+ T cells in both treatment groups (n=5 vehicle, n=8 MRTX-treated, unpaired t test, mean±SEM). Right: Percentage of naïve (CD44- CD62L+), effector (CD44+ CD62L-) and memory (CD44+ CD62L+) CD8+ T cells, same analysis as on the left for each cell population. (K) Contour plot of PD-1 and LAG-3 expression on CD8+ cells in vehicle and MRTX-treated 3LL ΔNRAS lung tumour samples (graph shows one representative example for n=5 vehicle and n=8 MRTX treated samples). (L) Visualization of cell outlines as measured by IMC, of CXCL9 negative and positive DCs, PD-1+ and LAG-3+ CD8+ T cells and regulatory T cells in a vehicle and a MRTX-treated tumour. (M) Quantification of occurrence of the different T cell subsets in the neighbourhood of CXCL9+ and CXCL9- DCs, depicted as the average proportion of that cell type among all neighbors within 100px radius of the DCs subset.

Figure 6

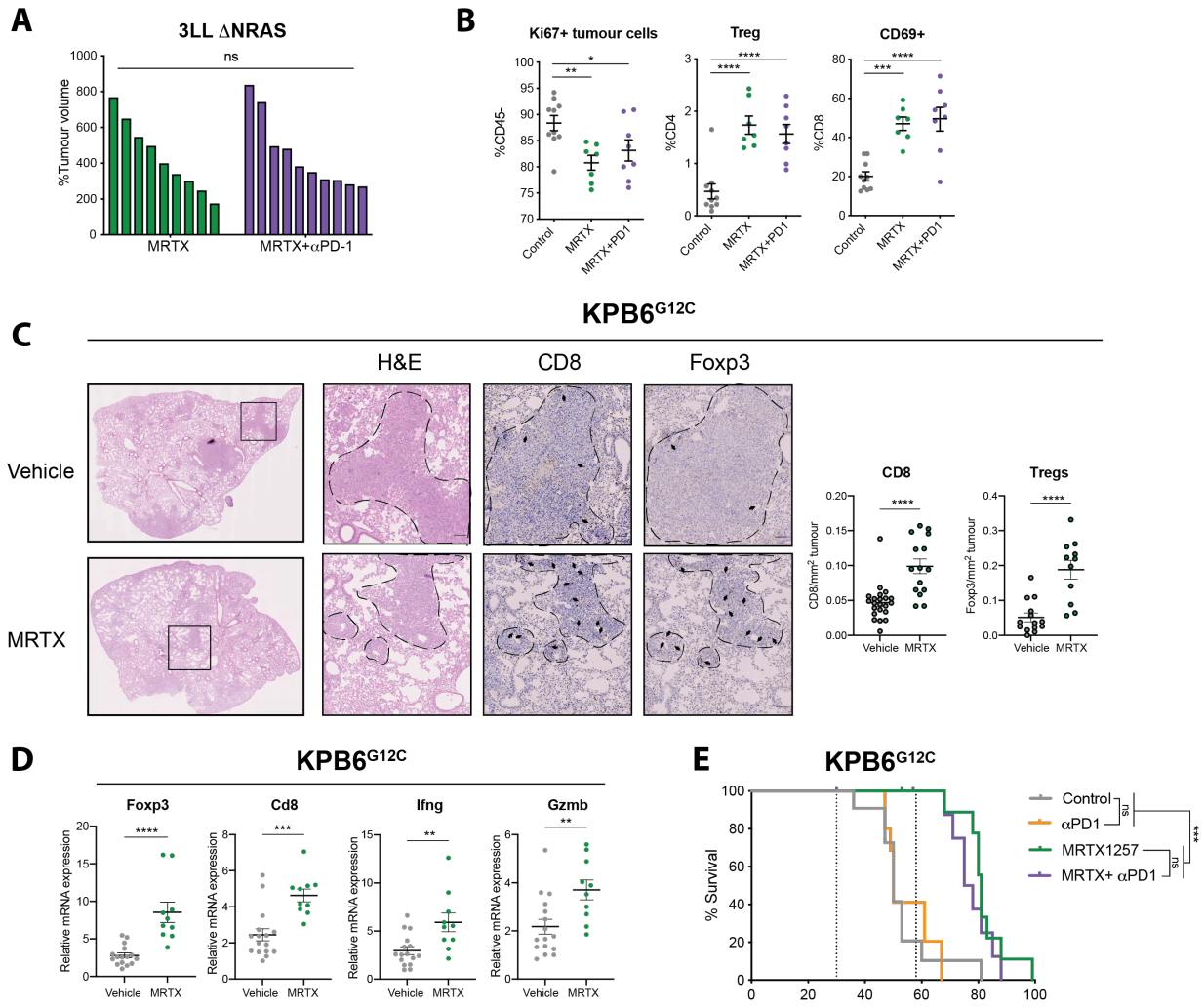

Fig. 6. KRAS^{G12C} inhibition does not synergize with ICB in immune refractory tumours. (A) Tumour volume change after two weeks of treatment of 3LL ΔNRAS-tumour bearing mice with either MRTX only (n=9 mice) or MRTX and anti-PD-1 (n=10 mice). (B) Flow cytometry analysis of proliferating tumour cells (CD45- Ki67+), Tregs (CD3+ CD4+ Foxp3+) and activated T cells (CD69+ CD8+) in vehicle (n=10), MRTX (n=7) or MRTX plus anti-PD1 (n=8) treated (two week treatment) 3LL ΔNRAS lung tumours (One way ANOVA, mean±SEM). (C) Immunohistochemistry analysis and quantification for CD8 (n=4 mice per group) and Foxp3 (n=3 mice per group) in KPB6^{G12C}-tumour bearing lungs after 7 days of vehicle or MRTX1257 treatment (each dot represents one tumour, unpaired t test, mean±SEM). (D) qPCR analysis of immune genes in vehicle (n=15 tumours) or MRTX-treated (n=10 tumours) KPB6^{G12C} lung tumours ($2^{-\Delta\Delta CT}$, Unpaired t test, mean±SEM). (E) Survival of KPB6^{G12C}lung tumour-bearing mice treated with vehicle (+IgG control, n=6 mice), MRTX1257 (+IgG control, n=6 mice), anti-PD-1 (n=5 mice) or combination (n=4 mice, Log-Rank Mantel Cox test).

Figure 7

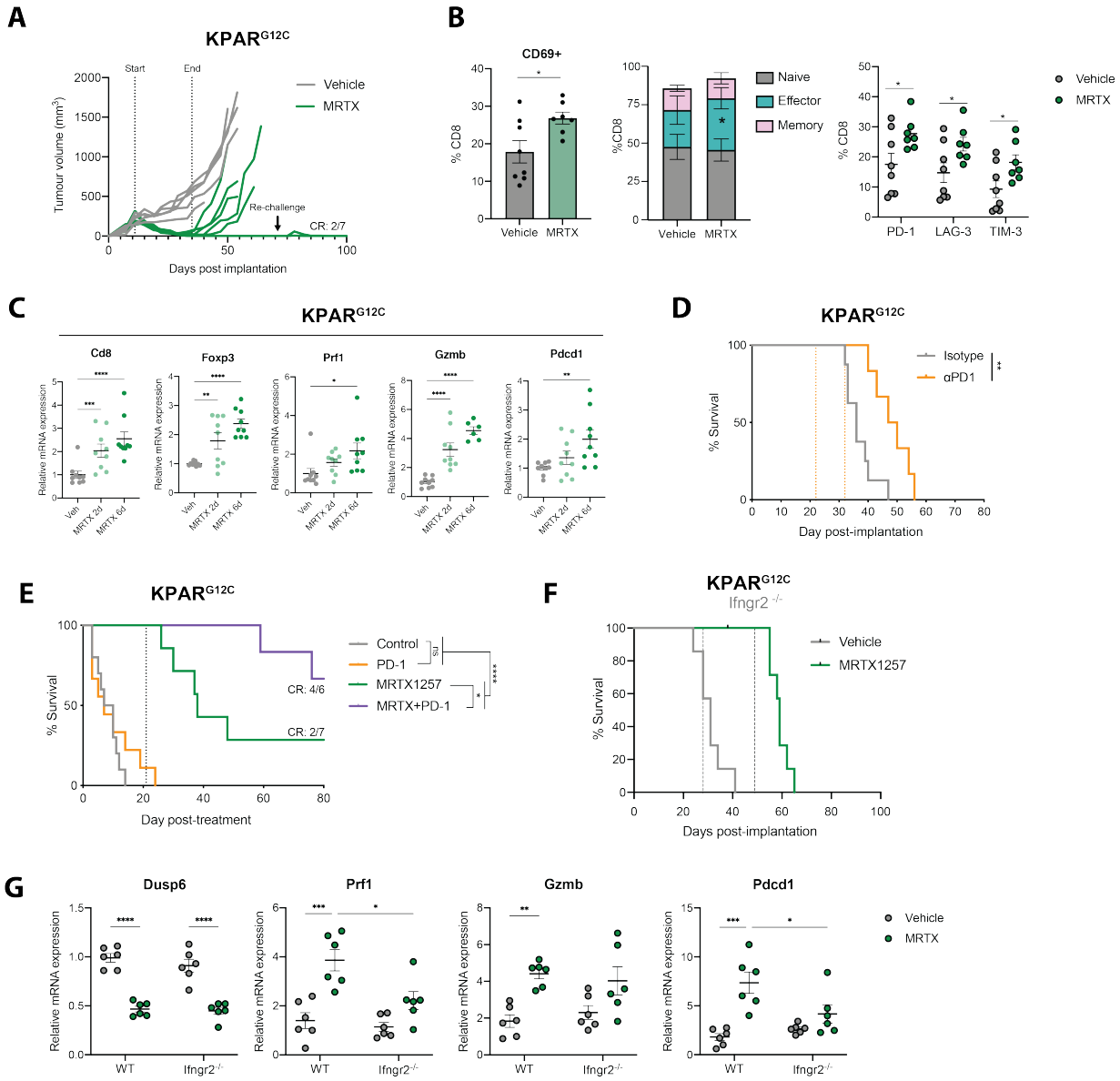

Fig. 7. In an immunogenic model, KRAS inhibition yields long-term responses, which are further improved by ICB. (A) Growth of subcutaneously implanted KPAR^{G12C}-tumours treated with either vehicle (Captisol) or 50mg/kg of MRTX849 for two weeks. At day 71, remaining mice were re-challenged with KPAR^{G12C} cells in the opposite flank, which did not give rise to tumours. (B) Flow cytometry analysis of KPAR^{G12C}-bearing lungs treated with either vehicle (n=8 mice) or 50mg/kg MRTX849 (n=7 mice) for 6 days, showing increased CD69+ CD8+ T cells (left), increased CD44+CD62L- effector CD8+ T cells (middle) and increased checkpoint molecule expression on CD8+ T cells (right) after KRAS inhibition (n=8 for control and n=6 for treated, all statistics are Student's t tests, mean±SEM). (C) qPCR analysis of KPAR^{G12C} lung tumours treated with vehicle or MRTX849 for two days or 6 days (n=3 mice per treatment group, 3 tumours per mouse). Each dot represents a lung tumour, one way ANOVA. (D)

Survival of KPAR^{G12C} lung tumour-bearing mice after treatment with IgG control (n=8 mice) or 10mg/kg anti-PD-1 (n=6 mice). Dotted lines represent start and end of treatment, respectively, Log-Rank Mantel Cox test. (E) Survival of KPAR^{G12C} lung tumour-bearing mice after treatment with Vehicle (+IgG control, n=6 mice), 10mg/kg anti-PD-1 (n=8 mice), 50mg/kg MRTX1257 (+ IgG control, n=4 mice) or both (n=6 mice). Dotted line represents end of treatment, Log-Rank Mantel Cox test. (F) Survival of KPAR^{G12C} *Ifngr2*$^{-/-}$ lung tumour-bearing mice after treatment with vehicle or 50mg/kg MRTX1257 (n=7 mice per group). Dotted lines represent treatment start and end, respectively, Log-Rank Mantel Cox test. (G) qPCR analysis of KPAR^{G12C} WT or *Ifngr2*$^{-/-}$ lung tumours treated with vehicle or MRTX1257 for 4 days (n=6 tumours per group, mean±SEM, $2^{-\Delta\Delta Ct}$). Each dot represents a lung tumour, one way ANOVA.